Synthesis, Structural Characterization, and Properties of New Single and Double Cubanes Containing the $MoFe_3S_4$ Structural Unit and Molybdenum-Bound Polycarboxylate Ligands. Clusters with a Molybdenum-Coordination Environment Similar to That in the Iron–Molybdenum Cofactor of Nitrogenase

Konstantinos D. Demadis and Dimitri Coucouvanis*

Department of Chemistry, The University of Michigan, Ann Arbor, Michigan 48109-1055

Received November 1, 1994[⊗]

The reaction of the previously characterized $(Et_4N)_2[MoFe_3S_4Cl_3(Cl_4\text{-cat})(CH_3CN)]$ (**1**) cluster with a variety of organic polycarboxylic acids, such as oxalic, citric, D-malic, *R*-citramalic, (methylimino)diacetic, or in some instances their salts ((Et$_4$N)(citrate)), affords in good yields $MoFe_3S_4$ cubanes with a Mo–polycarboxylate moiety. More specifically, the reaction of **1** with oxalic acid yields $(Et_4N)_4[(MoFe_3S_4Cl_4)_2(\mu\text{-}C_2O_4)]$, **3**. Cluster **3** crystallizes in the monoclinic space group *C2/c* with $a = 29.70(1)$ Å, $b = 12.462(3)$ Å, $c = 19.477(4)$ Å, $\beta = 155.76(2)°$, and $Z = 4$. The tetraanion consists of two $MoFe_3S_4$ cubane subunits linked by a bridging tetradentate oxalate through the Mo atoms. The Mo••Mo distance is found at 5.72 Å, and the Mo–Cl bond is 2.500(3) Å. The reaction of **3** with $(Et_4N)_2(C_2O_4)$ in CH_3CN gives $(Et_4N)_3[(MoFe_3S_4Cl_4)(C_2O_4)]$ (**4**) in moderate yields. **4** crystallizes in the monoclinic space group $P2_1/n$ with $a = 10.379(3)$ Å, $b = 22.682(8)$ Å, $c = 18.735(7)$ Å, $\beta = 92.21(1)°$, and $Z = 4$. The trianion core consists of a $MoFe_3S_4$ cubane possessing a terminal oxalate bound to the Mo atom. Upon reaction with $(Et_4N)CN$, **4** affords its Mo-bound cyano analog $(Et_4N)_3[(MoFe_3S_4Cl_3)(C_2O_4)(CN)]$ (**5**), which crystallizes in monoclinic space group $P2_1/n$ with $a = 10.331(2)$ Å, $b = 22.580(6)$ Å, $c = 19.083(4)$ Å, $\beta = 91.97(2)$ Å, and $Z = 4$. Metric features of **5** are similar to those of **4** with Mo–C and C–N bonds of 2.189(15) and 1.041(15) Å, respectively. Treatment of **4** with 0.5 equiv of $(Et_4N)CN$ followed by addition of $(Et_4N)SH$ affords the doubly-bridged double cubane $(Et_4N)_5\{[MoFe_3S_4Cl_2(C_2O_4)]_2(\mu_2\text{-CN})(\mu_2\text{-S})\}$ (**6**). Cluster **6** crystallizes in the monoclinic space group $P2_1/n$ with $a = 15.125(4)$ Å, $b = 21.254(7)$ Å, $c = 23.34(1)$ Å, $\beta = 94.62(3)°$, and $Z = 4$. The pentaanion consists of two $MoFe_3S_4$ cubane subunits having terminally Mo-bound bidentate oxalate and bridged by a μ_2-CN through the Mo atoms and a μ_2-S through two of the Fe atoms. Among the outstanding features in **6** are included long Mo••Mo and Fe••Fe(intercube) distances of 5.267(5) and 3.443(7) Å, respectively, and a Fe–μ_2-S–Fe angle of 104.1(4)°. The Mo–C, Mo–N, and C–N bond lengths are found at 2.25(3), 2.30(3), and 1.02(4) Å, respectively. The Mo–C(N)–N(C) angle of 157(3)° significantly diverges from linearity. Additionally, **1** reacts with (methylimino)diacetic acid to afford a cubane (**11**) with the same core structure and having the acid dianion coordinated to the Mo atom through its two carboxylate and imino N functions. Cluster **11** crystallizes in triclinic space group $P\bar{1}$ with $a = 10.356(3)$ Å, $b = 11.506(4)$ Å, $c = 15.474(7)$ Å, $\alpha = 98.14(3)°$, $\beta = 100.64(3)°$, $\gamma = 92.02(3)°$, and $Z = 2$. The electrochemical properties, spectroscopic characteristics, and reactivity of the new clusters are discussed.

Introduction

In nature the activation and reduction of dinitrogen to ammonia is catalyzed by nitrogenase.[1] This complex enzyme contains two component proteins of which the Fe protein[1a] (M_r = 63 kD) serves as a source of electrons for the substrate-reducing FeMo protein (M_r = 230 kD). The FeMo protein contains 30 Fe and 2 Mo atoms that are distributed in two Fe_7MoS_{8-9} clusters and two Fe_8S_{7-8} clsuters (P-clusters). The Fe/Mo/S sites are believed to be intimately connected with the biological reduction of dinitrogen to ammonia (with the concomitant reduction of protons) (eq 1) and also with the multielectron reduction of various other substrates. The remarkable reactivity of the Fe/Mo/S center in nitrogenase accounts for the intense interest in the FeMo protein and the isolated

$$N_2 + 8e^- + 8H^+ + 16MgATP \rightarrow 2NH_3 + H_2 + 16MgADP + 16P_i \quad (1)$$

Fe/Mo/S center[2] (FeMo-co) that has resulted in numerous genetic,[3] biochemical,[4] analytical,[5] and spectroscopic[6–12] studies.

Recent single crystal X-ray structure determinations of the Fe–Mo protein of nitrogenase from *A. vinelandii*[13] and *C. pasteurianum*[13,14] have revealed the structure of the Fe/Mo/S

[⊗] Abstract published in *Advance ACS Abstracts,* December 15, 1994.

[1] (a) Stiefel, E. I.; Coucouvanis, D.; Newton, W. E. *Molybdenum Enzymes,* Cofactors and Model Systems; ACS Symposium Series 535; American Chemical Society: Washington, DC, 1993; Chapers 10–23. (b) Dilworth, M. J.; Glenn, A. P. *Biology and Biochemistry of Nitrogen Fixation*; Elsevier: Amsterdam, 1991. (c) Stacey, G.; Burris, R. H.; Evans, H. J. *Biological Nitrogen Fixation*; Chapman and Hall: New York, 1992.

[2] Shah, V. K.; Brill, W. J. *Proc. Natl. Acad. Sci. U.S.A.* **1977**, *74*, 3249.

[3] (a) Orme-Johnson, W. H. *Annu. Rev. Biophys. Biophys. Chem.* **1985**, *14*, 419. (b) Hoover, T. R.; Imperial, J.; Ludden, P. W.; Shah, V. K. *Biofactors* **1988**, *1*, 199.

[4] (a) Burgess, B. K. In *Advances in Nitrogen Fixation Research*; Veeger, C., Newton, W. E., Eds.; Nijhoff-Junk-Pudoc: Dordrecht, The Netherlands, 1983; p 103. (b) Nelson, M. J.; Lindahl, P. A.; Orme-Johnson, W. H. *Adv. Inorg. Biochem.* **1982**, *4*, 1. (c) Burgess, B. K.; Newton, W. E. In *Nitrogen Fixation: The Chemical-Biochemical-Genetic Interface*; Muller, A., Newton, W. E., Eds.; Plenum Press: New York, 1983; p 83. (d) Burgess, B. K. In *Nitrogen Fixation Research Progress*; Evans, H. J., Bottomley, P. J., Newton, W. E., Eds.; Martinus Nijhoff Publishers: Dordrecht, The Netherlands, 1985; p 543. (e) Burgess, B. K. In *Molybdenum Enzymes*; Spiro, T. G., Ed.; John Wiley and Sons: New York, 1985; p 161. (f) Burgess, B. K. *Chem. Rev.* **1990**, *90*, 1377.

0020-1669/95/1334-0436$09.00/0

aggregate to near atomic resolution. The Fe/Mo/S cluster (Figure 1) consists of two cuboidal subunits, Fe_4S_3 and $MoFe_3S_3$, bridged by two[13] or three[14] S^{2-} ions and anchored on the protein matrix by a Fe-coordinated cysteinyl residue and by a Mo-coordinated imidazole group from a histidine residue. The Mo atom also is coordinated by a homocitrate molecule that serves as a bidentate chelate through the central carboxylate and the hydroxyl groups. Unusual structural features in the Fe/Mo/S center include the unprecedented trigonal planar coordination geometry for the six μ-S-bridged iron atoms and the unusually short Fe−Fe distances across the two subunits (2.5−2.6 Å).

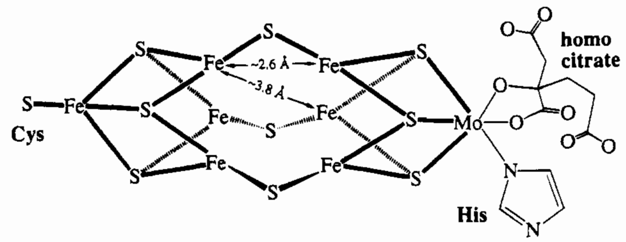

Figure 1. Schematic representation of the Fe/Mo/S center in nitrogenase.[13]

The presence of homocitrate as an *integral* component of the FeMo-co had been demonstrated earlier by Ludden *et al.*,[15] who also replaced the homocitrate ligand by a plethora of alternative polycarboxylic acids by *in vitro* syntheses of the FeMo-co.[16] A few of these carboxylic acids including citric, malic, citramalic, and citroylformic displayed N_2 reduction activity well above the background limits.[17] This activity still was much lower than that found with homocitrate. The experimental evidence from this structure/function investigation led to several conclusions[18] including the following: (i) A hydroxyl group (or in some instances a keto group) and a minimum of two carboxyl groups are required for activity. (ii) the (*R*) isomers of the organic acids are greatly preferred to the (*S*) acids. (iii) The minimum organic acid that will support synthesis of a functional entity is malate (with D as the preferred configuration). In spite of the large volume of information available, it is not known whether homocitrate directly participates in substrate reduction (as a possible proton donor for example) or it simply serves as a ligand for the Mo.

During the last decade a large number of synthetic Mo/Fe/S clusters have been synthesized and characterized.[19] Predominant among these clusters are those that contain as a common structural feature one[20] or two[21] $MoFe_3S_4$ "cubane" structural units. The latter have been the focus of extensive spectroscopic and reactivity[22] studies. The $[MoFe_3S_4L_3(R\text{-cat})(L')]^{n-}$ clusters[20] (R-cat = substituted catechol, L = thiolate or halide

---

(5) (a) Nelson, M. J.; Levy, M. A.; Orme-Johnson, W. H. *Proc. Natl. Acad. Sci. U.S.A.* **1983**, *80*, 147. (b) Burgess, B. K.; Jacobs, D. R.; Stiefel, E. I. *Bioch. Biophys. Acta* **1980**, *614*, 196. (c) Yang, S. S.; Pan, W. H.; Friesen, G. D.; Burgess, B. K.; Corbin, J. L.; Newton, W. E. *J. Biol. Chem.* **1982**, *257*, 8042. (d) Stiefel, E. I.; Cramer, S. P. In *Molybdenum Enzymes*; Spiro, T. G., Ed.; John Wiley and Sons: New York, 1985; p 89. (e) Frank, P.; Gheller, S. F.; Newton, W. E.; Hodgson, K. O. *Biochem. Biophys. Res. Commun.* **1989**, *163*, 746. (f) McLean, P. A.; Wink, D. A.; Chapman, S. K.; Hickman, A. B.; McKillop, D. M.; Orme-Johnson, W. H. *Biochemistry* **1989**, *28*, 9402. (g) Wink, D. A.; McLean, P. A.; Hickman, A. B.; Orme-Johnson, W. H. *Biochemistry* **1989**, *28*, 9407.

(6) Mössbauer studies: (a) Zimmerman, R.; Munck, E.; Brill, W. J.; Shah, V. K.; Henzl, M. T.; Rawlings, J.; Orme-Johnson, W. H. *Biochim. Biophys. Acta* **1978**, *537*, 185. (b) Huynh, B. H.; Munck, E.; Orme-Johnson, W. H. *Biochim. Biophys. Acta* **1979**, *576*, 192. (c) Huynh, B. H.; Henzl, M. T.; Christner, J. A.; Zimmerman, R.; Orme-Johnson, W. H.; Munck, E. *Biochim. Biophys. Acta* **1980**, *623*, 124. (d) McLean, P. A.; Papaefthymiou, V.; Orme-Johnson, W. H.; Munck, E. *J. Biol. Chem.* **1987**, *262*, 12900. (e) Lindahl, P. A.; Papaefthymiou, V.; Orme-Johnson, W. H.; Munck, E. *J. Biol. Chem.* **1988**, *263*, 19412. (f) Smith, B. E.; O'Donnell, M. J.; Lang, G.; Spartalian, K. *Biochem. J.* **1980**, *191*, 449. (g) Dunham, W. R.; Hagen, W. R.; Braaksma, A.; Grande, H. J.; Haaker, H. *Eur. J. Biochem.* **1985**, *146*, 497. (h) Newton, W. E.; Gheller, S. F.; Sands, R. H.; Dunham, W. R. *Biochem. Biophys. Res. Commun.* **1989**, *162*, 882.

(7) Electron paramagnetic resonance studies: (a) Hoffman, B. M.; Venters, R. A.; Roberts, J. E.; Nelson, M.; Orme-Johnson, W. H. *J. Am. Chem. Soc.* **1982**, *104*, 4711. (b) Hoffman, B. M.; Roberts, J. E.; Orme-Johnson, W. H. *J. Am. Chem. Soc.* **1982**, *104*, 860. (c) Thomann, H.; Morgan, T. V.; Jin, H.; Burgmayer, S. J. N.; Bare, R. E.; Stiefel, E. I. *J. Am. Chem. Soc.* **1987**, *109*, 7913. (d) True, A. E.; Nelson, M. J.; Venters, R. A.; Orme-Johnson, W. H.; Hoffman, B. M. *J. Am. Chem. Soc.* **1988**, *110*, 1935. (e) Euler, W. B.; Martinsen, J.; McDonald, J. W.; Watt, G. D.; Wang, Z.-C. *Biochemistry* **1984**, *23*, 3021. (f) George, G. N.; Bare, R. E.; Jin, H.; Stiefel, E. I.; Prince, R. C. *Biochem. J.* **1989**, *262*, 349.

(8) EXAFS studies: (a) Cramer, S. P.; Hodgson, K. O.; Gillum, W. O.; Mortenson, L. E. *J. Am. Chem. Soc.* **1978**, *100*, 3398. (b) Cramer, S. P.; Gillum, W. O.; Hodgson, K. O.; Mortenson, L. E.; Stiefel, E. I.; Chisnell, J. R.; Brill, W. J.; Shah, V. K. *J. Am. Chem. Soc.* **1978**, *100*, 3814. (c) Flank, A. M.; Weininger, M.; Mortenson, L. E.; Cramer, S. P. *J. Am. Chem. Soc.* **1986**, *108*, 1049. (d) Condradson, S. D.; Burgess, B. K.; Newton, W. E.; Mortenson, L. E.; Hodgson, K. O. *J. Am. Chem. Soc.* **1987**, *109*, 7507. (e) Hedman, B.; Frank, P.; Gheller, S. F.; Roe, A. L.; Newton, W. E.; Hodgson, K. O. *J. Am. Chem. Soc.* **1988**, *110*, 3798. (f) Condradson, S. D.; Burgess, B. K.; Vaughn, S. A.; Roe, A. L.; Hedman, B.; Hodgson, K. O.; Holm, R. H. *J. Biol. Chem.* **1989**, *264*, 15967. (g) Condradson, S. D.; Burgess, B. K.; Newton, W. E.; Hodgson, K. O.; McDonald, J. W.; Rubinson, J. F.; Gheller, S. F.; Mortenson, L. E.; Adams, M. W. W.; Mascharak, P. D.; Armstrong, W. A.; Holm, R. H. *J. Am. Chem. Soc.* **1985**, *107*, 7935. (h) Antonio, M. R.; Averill, B. A.; Groh, S. E.; Kauzlarich, S. M.; Lindahl, P. A.; Nelson, M. J.; Orme-Johnson, W. H.; Teo, B.-K. *J. Am. Chem. Soc.* **1982**, *104*, 4703. (i) Arber, J. M.; Flood, A. C.; Garner, C. D.; Gormal, C. A.; Hasnain, S. S.; Smith, B. E. *Biochem. J.* **1988**, *252*, 421.

(9) Magnetic susceptibility studies: (a) Smith, J. P.; Emptage, M. H.; Orme-Johnson, W. H. *J. Biol. Chem.* **1982**, *257*, 2310. (b) Day, E. P.; Kent, T. A.; Lindahl, P. A.; Munk, E.; Orme-Johnson, W. H.; Roder, H.; Roy, A. *Biophys. J.* **1987**, *52*, 837.

(10) Magnetic circular dichroism studies: (a) Stephens, P. J.; McKenna, C. E.; Smith, B. E.; Nguyen, H. T.; McKenna, M. C.; Thomson, A. J.; Devlin, F.; Jones, J. B. *Proc. Natl. Acad. Sci. U.S.A.* **1979**, *76*, 2585. (b) Stephens, McKenna, C. E.; McKenna, M. C.; Nguyen, H. T.; Devlin, F. *Biochemistry* **1981**, *20*, 2857. (c) Johnson, M. K.; Thomson, A. J.; Robinson, A. E.; Smith, B. E. *Biochim. Biophys. Acta* **1981**, *671*, 61.

(11) ENDOR studies: Hoffman, B. M.; Venters, R. A.; Roberts, J. E.; Nelson, M.; Orme-Johnson, W. H. *J. Am. Chem. Soc.* **1982**, *104*, 4711.

(12) Nuclear magnetic resonance studies: (a) Mascharak, P. K.; Smith, M. C.; Armstrong, W. H.; Burgess, B. K.; Holm, R. H. *Proc. Natl. Acad. Sci. U.S.A.* **1982**, *79*, 7056. (b) Condradson, S. D.; Burgess, B. K.; Holm, R. H. *J. Biol. Chem.* **1988**, *263*, 13743.

(13) (a) Kim, J.; Rees, D. C. *Science* **1992**, *257*, 1677. (b) Kim, J.; Rees, D. C. *Nature* **1992**, *360*, 553. (c) Kim, J.; Woo, D.; Rees, D. C. *Biochemistry* **1993**, *32*, 7104. (d) Chan, M. K.; Kim, J.; Rees, D. C. *Science* **1993**, *260*, 792. (e) Kim, J.; Rees, D. C. *Biochemistry* **1994**, *33*, 389. (f) Reference 1a, p 170.

(14) (a) Bolin, J. T.; Ronco, A. E.; Morgan, T. V.; Mortenson, L. E.; Xuong, N. H. *Proc. Natl. Acad. Sci. U.S.A.* **1993**, *90*, 1078. (b) Bolin, J. T.; Campobasso, N.; Muchmore, s. W.; Minor, W.; Morgan, T. V.; Mortenson, L. E. In *New Horizons in Nitrogen Fixation*; Palacios, P., Moura, J., Newton, W. W., Eds.; Kluwer: Dordrecht, The Netherlands, 1993; p 83. (c) Reference 1a, p 186.

(15) (a) Hoover, T. R.; Shah, V. K.; Roberts, G. P.; Ludden, P. W. *J. Bacteriol.* **1986**, *167*, 999. (b) Hoover, T. R.; Robertson, A. D.; Cerny, R. L.; Hayes, R. N.; Imperial, J.; Shah, V. K.; Ludden, P. W. *Nature* **1987**, *329*, 855. (c) Hoover, T. R.; Imperial, J.; Ludden, P. W.; Shah, V. K. *Biochemistry* **1989**, *28*, 2768.

(16) (a) Hoover, T. R.; Imperial, J.; Liang, J.; Ludden, P. W.; Shah, V. K. *Biochemistry* **1988**, *27*, 3647. (b) Imperial, J.; Hoover, T. R.; Madden, M. S.; Ludden, P. W.; Shah, V. K. *Biochemistry* **1989**, *28*, 7796. (c) Madden, M. S.; Kindon, N. D.; Ludden, P. W.; Shah, V. K. *Proc. Natl. Acad. Sci. U.S.A.* **1990**, *87*, 6517. (d) Liang, J.; Madden, M. S.; Shah, V. K.; Burris, R. H. *Biochemistry* **1990**, *29*, 8577.

(17) (a) Hoover, T. R.; Imperial, J.; Ludden, P. W.; Shah, V. K. *J. Bacteriol.* **1988**, *170*, 1978. (b) Madden, M. S.; Paustian, T. D.; Ludden, P. W.; Shah, V. K. *J. Bacteriol.* **1991**, *173*, 5403.

(18) Reference 1a, p 196.

(19) (a) Holm, R. H.; Simhon, E. D. In *Molybdenum Enzymes*; Spiro, T. G., Ed.; Wiley-Interscience: New York, 1985; p 1. (b) Coucouvanis, D. *Acc. Chem. Res.* **1991**, *24*, 1. (c) Eldredge, P. A.; Bose, K. S.; Barber, D. E.; Bryan, R. F.; Sinn, E.; Reingold, A.; Averill, B. A. *Inorg. Chem.* **1991**, *30*, 2365.

ligands, L′ = coordinating solvent or other neutral or anionic ligands) are of particular significance as structural analogs for the Mo subsite within the Fe/Mo/S center.[19a] The analogy stems from the first and second coordination sphere environments around the Mo atoms that are very similar the Mo environment in the native Fe/Mo/S center (Figure 1) and from the cluster spin ground state[23] ($S = {}^3/_2$) that mimics the semireduced state of the Fe–Mo protein of nitrogenase and of the extruded FeMo-co. In our studies we have been using the $[MoFe_3S_4Cl_3(Cl_4\text{-cat})(L)]^{2-}$ cluster[20d] (L = coordinating solvent molecule), **1**, as a reagent for reactivity studies. Additional characteristics of this cluster that are appealing from a synthetic and reactivity point of view are as follows: (i) The Mo-bound, bidentate, Cl_4-cat ligand can be protonated readily by conjugate acids of potential ligands, and (ii) there is the presence of chlorides as Fe-bound terminal ligands that, unlike thiolate ligands, are unreactive toward polycarboxylic or other moderately strong acids.

We have explored the synthetic utility of **1** in the synthesis of other derivative clusters by allowing it to react with a variety of dicarboxylic and hydroxy–polycarboxylic acids. Preliminary findings of this study have been communicated earlier.[24] In this paper we provide extensive documentation on the synthesis, molecular structures, and spectroscopic properties of these first examples of $MoFe_3S_4$ clusters that contain Mo-coordinated polycarboxylate anions. Preliminary reactivity studies of the clusters reported herein show these molecules to be catalytically active. Such studies are expected to be important for an understanding of the role that specific structural and electronic features of Mo-bound carboxylate ligands play in catalysis.

Experimental Section

Synthesis. All experimental procedures were conducted under strictly anaerobic conditions using either a Vacuum Atmospheres Dri-Lab glovebox filled with prepurified nitrogen or standard Schlenk techniques. The chemicals in this research were used as purchased, except the solvents, which were purified as follows: Acetonitrile (CH_3CN) and dichloromethane (CH_2Cl_2) were distilled over calcium hydride (CaH_2) before use. Diethyl ether (Et_2O) was distilled over Na and benzophenone. Ethanol, methanol, and acetone were stored over 4 Å Linde molecular sieves. All the solvents were degassed with a stream of prepurified N_2 prior to use. All the carboxylic acids, NaSH, Li_2S, and $(Et_4N)CN$ were purchased from Aldrich Chemical Co. and used without further purification. Anhydrous $(Et_4N)Cl$ was purchased from Eastman Kodak. A 25% methanolic solution of $(Et_4N)OH$ was purchased from Fluka. Elemental analyses were performed by the Analytical Services Laboratory in the Department of Chemistry at the University of Michigan.

Physical Methods. Electronic spectra were recorded on a Cary 1E (Varian) spectrophotometer. Mid-infrared spectra were collected on a Nicolet 5-DX FT-IR spectrophotometer at a 4 cm^{-1} resolution and far-infrared spectra were obtained on a Nicolet 740 FT-IR spectrophotometer, both in CsI disks. Electrochemical studies were performed with a BAS electroanalyzer. The electrochemical cell used had a platinum disk as the working electrode, a Pt wire as the auxiliary one, and an Ag/AgCl electrode as the reference one. All solvents used in the electrochemical experiments were properly distilled and deaerated (by purging with a stream of Ar). Tetra-*n*-butylammonium perchlorate (Bu_4NClO_4) was utilized as the supporting electrolyte. Typical concentrations used were $\sim 10^{-3}$ M in electroanalyte and 10^{-2} M in supporting electrolyte.

Preparation of Compounds. $(Et_4N)_2[MoFe_3S_4Cl_3(Cl_4\text{-cat})(CH_3CN)]$,[25] 1, and $(Et_4N)_4[Mo_2Fe_6S_8(SEt)_6(Cl_4\text{-cat})_2]$, 2, were synthesized by a modified published procedure.[20d]

$(Et_4N)_2(C_2O_4)$. Anhydrous oxalic acid (2.00 g, 22.20 mmol) was dissolved in methanol (~20 mL), and to the solution was added dropwise a 25% w/w methanolic solution of $(Et_4N)OH$ (26.17 g, 44.40 mmol) via a pressure-equalizing funnel, over a period of ~1 h. The resulting clear colorless solution was taken to dryness to afford a viscous liquid, which was recrystallized from CH_3CN/Et_2O. A white powder was obtained which was washed thoroughly with Et_2O and dried *in vacuo* at 55 °C (yield 6.00 g, 78%). The product was extremely hygroscopic and was therefore stored in the glovebox. It was used without any further purification. Mid-infrared spectrum: $\nu(C{=}O)$, 1550 (vs, br) cm^{-1}. No residual $\nu(O{-}H)$ was detected.

(Et_4N)(citrate). Anhydrous citric acid (2.00 g, 10.40 mmol) was dissolved in ~20 mL of methanol. To this clear solution, a 25% w/w methanolic solution of $(Et_4N)OH$ (6.13 g, 10.40 mmol) was added dropwise via a pressure-equalizing funnel over a period of 2 h. The solution was stirred for 12 h and then evaporated to dryness. A white powder was isolated and recrystallized from hot CH_3CN. A white highly crystalline material was obtained after standing at −20 °C for ca. 12 h (yield 3.20 g, 95%). This solid was dried *in vacuo* at 50 °C and was used without further purification. Anal. Calcd for $C_{14}H_{27}O_7N$ (MW 321.38): C, 52.27; H, 8.40; N, 4.36. Found: C, 53.23; H, 8.69; N, 4.40. Mid-infrared spectrum: $\nu(C{=}O)$ 1578 (vs), 1721 (vs), 1975 (m, br) cm^{-1}; $\nu(O{-}H)$ 3402 (m, br) cm^{-1}.

$(Et_4N)SH$. This compound was obtained by mixing NaSH and anhydrous $(Et_4N)Cl$ in 1:1 ratio in degassed ethanol. After removal of NaCl by filtration the filtrate was taken to dryness. The solid was recrystallized from a CH_3CN/Et_2O mixture to give a white powder. Alternatively, $(Et_4N)SH$ is generated (via Hoffmann elimination) upon mixing Et_4NCl and Li_2S in ethanol in a 2:1 molar ratio. Anal. Calcd for $C_8H_{21}NS{\cdot}H_2O$ (MW 181.32): C, 52.94; H, 11.58; N, 7.72. Found: C, 51.80; H, 11.38; N, 7.56. Infrared spectrum: $\nu(S{-}H)$, 2551, 2575 (w) cm^{-1}.

$(Et_4N)_4[(MoFe_3S_4Cl_4)_2(\mu\text{-}C_2O_4)]$ (3). An amount of **1** (1.00 g, 0.96 mmol) was mixed with $(Et_4N)Cl$ (0.16 g, 0.96 mmol) in 30 mL of CH_3CN giving a brown-orange solution. To this solution a 0.1 M stock solution of oxalic acid in CH_3CN (10 mL, 0.96 mmol) was added dropwise via syringe over a period of 10 min, during which the color changed to darker brown. After 20 min of further stirring, the solution was filtered (no residue). Slow addition of Et_2O (80 mL) to the filtrate

---

(20) (a) Mizobe, Y.; Mascharak, P. K.; Palermo, R. E.; Holm, R. H. *Inorg. Chim. Acta* **1983**, *80*, L65. (b) Mascharak, P. K.; Armstrong, W. H.; Mizobe, Y.; Holm, R. H. *J. Am. Chem. Soc.* **1983**, *105*, 475. (c) Palermo, R. E.; Holm, R. H. *J. Am. Chem. Soc.* **1983**, *105*, 4310. (d) Palermo, R. E.; Singh, R.; Bashkin, J. K.; Holm, R. H. *J. Am. Chem. Soc.* **1984**, *106*, 2600. (e) Zhang, Y. P.; Bashkin, J. K.; Holm, R. H. *Inorg. Chem.* **1987**, *26*, 694. (f) Liu, Q.; Huang, L.; Liu, H.; Lei, X.; Wu, D.; Kang, B.; Lu, J. *Inorg. Chem.* **1990**, *29*, 4131.

(21) (a) Wolff, T. E.; Berg, J. M.; Hodgson, K. O.; Frankel, R. B.; Holm, R. H. *J. Am. Chem. Soc.* **1979**, *101*, 4140. (b) Wolff, T. E.; Power, P. P.; Frankel, R. B.; Holm, R. H. *J. Am. Chem. Soc.* **1980**, *102*, 4694. (c) Palermo, R. E.; Power, P. P.; Holm, R. H. *Inorg. Chem.* **1982**, *21*, 173. (d) Wolff, T. E.; Berg, J. M.; Power, P. P.; Hodgson, K. O.; Holm, R. H. *Inorg. Chem.* **1980**, *19*, 430. (e) Armstrong, W. H.; Mascharak, P. K.; Holm, R. H. *J. Am. Chem. Soc.* **1982**, *104*, 4373. (f) Coucouvanis, D.; Challen, P. R.; Koo, S. M.; Davis, W. M.; Butler, W.; Dunham, W. R. *Inorg. Chem.* **1989**, *28*, 4181. (g) Challen, P. R.; Koo, S. M.; Kim, C. G.; Dunham, W. R.; Coucouvanis, D. *J. Am. Chem. Soc.* **1990**, *112*, 8606.

(22) (a) Tanaka, M.; Tanaka, K.; Tanaka, T. *Chem. Lett.* **1982**, 767. (b) Tanaka, K.; Hozumi, Y.; Tanaka, T. *Chem. Lett.* **1982**, 1203. (c) Tanaka, K.; Imasaka, Y.; Tanaka, M.; Honjo, M.; Tanaka, T. *J. Am. Chem. Soc.* **1982**, *104*, 4258. (d) Komeda, N.; Nagao, H.; Matsui, T.; Adachi, G.; Tanaka, K. *J. Am. Chem. Soc.* **1992**, *114*, 3625.

(23) (a) Armstrong, W. H.; Holm, R. H. *J. Am. Chem. Soc.* **1981**, *103*, 6246. (b) Mascharak, P. K.; Papaefthymiou, G. C.; Armstrong, W. H.; Foner, S.; Frankel, R. B.; Holm, R. H. *Inorg. Chem.* **1983**, *22*, 2851.

(24) (a) Coucouvanis, D.; Demadis, K. D.; Kim, C. G.; Dunham, R. W.; Kampf, J. W. *J. Am. Chem. Soc.* **1993**, *115*, 3344. (b) Demadis, K. D.; Chen, S. J.; Coucouvanis, D. *Polyhedron* **1994**, in press.

(25) For comparison reasons we present some spectroscopic data we have obtained on this compound. Electronic spectrum (CH_3CN): λ_{max} 470 (sh), 300 (sh), nm. Far-infrared spectrum: 268 (w), 300 (m), 315 (w), 346 (vs), 361 (s), 383 (sh), 395 (w), 411 (m), 425 (w) cm^{-1}. Mid-infrared spectrum: $\nu(C{\equiv}N)$ (Mo-bound CH_3CN) 2284 (w), 2312 (w) cm^{-1}; Cl_4-cat 1255 (s), 805 (s) cm^{-1}; Mo–O(Cl_4-cat) 542 (m) cm^{-1}. Abbreviations used in text: Cl_4-cat = tetrachlorocatecholate dianion, Hcit = citrate trianion, H_2cit = citrate dianion, Hcmal = citramalate dianion, Hmal = malate dianion, mida = methyliminodiacetate dianion.

caused precipitation of a black microcrystalline solid. This material was collected by filtration, washed with methanol and $\mathrm{Et_2O}$, and dried *in vacuo* (yield 0.76 g, 95%). Electronic spectrum ($\mathrm{CH_3CN}$): $\lambda_{\max}$ (ϵ_M) 570 (3080), 475 (5250). Anal. Calcd for $\mathrm{Mo_2Fe_6Cl_8S_8O_4N_4C_{34}H_{80}}$ (**3**, MW 1676.11): C, 24.34; H, 4.77; N, 3.34. Found: C, 25.20; H, 4.86; N, 3.34. Far-infrared spectrum: 278 (w), 314 (m), 323 (m), 358 (vs), 398 (sh), 413 (m), 465 (w) $\mathrm{cm^{-1}}$. Mid-infrared spectrum: $\nu_{\mathrm{asym}}(\mathrm{C{=}O})$ 1635 (vs), 1667 (m), 1695 (w) $\mathrm{cm^{-1}}$; $\nu_{\mathrm{sym}}(\mathrm{C{-}O})$ 1460 $\mathrm{cm^{-1}}$.

$(\mathrm{Et_4N})_3[(\mathrm{MoFe_3S_4Cl_4})(\mathrm{C_2O_4})]$ (4). An amount of **3** (0.50 g, 0.30 mmol) was dissolved in a minimum amount of $\mathrm{CH_3CN}$ (~10 mL). To this solution, a solution of $(\mathrm{Et_4N})_2(\mathrm{C_2O_4})$ (0.12 g, 0.36 mmol) in 20 mL of $\mathrm{CH_3CN}$ was added *dropwise* with vigorous stirring over a period of 1 h. The mixture gradually turned darker brown with a reddish cast, and formation of an insoluble material was observed. After 2 h of additional stirring the mixture was filtered to remove the brown-black insoluble material, which was discarded. Slow addition of $\mathrm{Et_2O}$ (70 mL) to the filtrate afforded a highly crystalline material as black needles (yield 0.33 g, 55%). Electronic spectrum ($\mathrm{CH_3CN}$): $\lambda_{\max}$ (ϵ_M) 450 (6420), 310 (13 600) nm. Anal. Calcd for $\mathrm{MoFe_3Cl_4S_4O_4N_3C_{26}H_{60}}$ (**4**, MW 1011.53): C, 30.84; H, 5.93; N, 4.15. Found: C, 30.91; H, 5.97; N, 4.10. Far-infrared spectrum: 278 (w), 309 (w), 324 (m), 352 (vs), 392 (w), 412 (m) $\mathrm{cm^{-1}}$. Mid-infrared spectrum: $\nu_{\mathrm{asym}}(\mathrm{C{=}O})$ 1637 (m), 1667 (vs), 1698 (w) $\mathrm{cm^{-1}}$; $\nu_{\mathrm{sym}}(\mathrm{C{-}O})$ 1378 (m) $\mathrm{cm^{-1}}$.

$(\mathrm{Et_4N})_3[\mathrm{MoFe_3S_4Cl_3(C_2O_4)(CN)}]$ (5). An amount of **4** (0.20 g, 0.20 mmol) was dissolved in 30 mL $\mathrm{CH_3CN}$ and to it was added a solution of $(\mathrm{Et_4N})\mathrm{CN}$ (0.03 g, 0.20 mmol, in 5 mL of $\mathrm{CH_3CN}$). The dark brown solution was stirred for 3 h and then filtered to remove a negligible amount of a black residue. Addition of $\mathrm{Et_2O}$ (50 mL) to the filtrate caused the precipitation of a highly crystalline material (black needles). This was isolated, washed with MeOH, acetone, and $\mathrm{Et_2O}$, and dried *in vacuo* (yield 0.18 g, 90%). Electronic spectrum ($\mathrm{CH_3CN}$): $\lambda_{\max}$ (ϵ_M) 420 (2300), 320 (5400), and 240 (14 100) nm. Anal. Calcd for $\mathrm{MoFe_3S_4Cl_3C_{27}H_{60}N_4O_4}$ (**5**, MW 1002.08): C, 32.33; H, 5.99; N, 5.52. Found: C, 32.39; H, 6.09; N, 5.51. Far-infrared spectrum: 266 (m), 318 (m), 341 (vs), 355 (vs), 374 (sh), 391 (w), 414 (m), 450 (w) $\mathrm{cm^{-1}}$. Mid-infrared spectrum: $\nu(\mathrm{C{\equiv}N})$ 2123 (w) $\mathrm{cm^{-1}}$, $\nu_{\mathrm{asym}}(\mathrm{C{=}O})$ 1639 (s), 1673 (vs), 1700 (s) $\mathrm{cm^{-1}}$, $\nu_{\mathrm{sym}}(\mathrm{C{-}O})$ 1378 (s) $\mathrm{cm^{-1}}$.

$(\mathrm{Et_4N})_5\{[\mathrm{MoFe_3S_4Cl_2(C_2O_4)}]_2(\mu\text{-}\mathrm{S})(\mu\text{-}\mathrm{CN})\}$ (6). Method A. An amount of **3** (0.20 g, 0.12 mmol) was dissolved in 30 mL of $\mathrm{CH_3CN}$. To this solution, a mixture of $(\mathrm{Et_4N})_2(\mathrm{C_2O_4})$ (0.042 g, 0.12 mmol), $(\mathrm{Et_4N})\mathrm{CN}$ (0.01 g, 0.06 mmol), and $(\mathrm{Et_4N})\mathrm{SH}$ (0.02 g, 0.10 mmol) dissolved in ~10 mL of $\mathrm{CH_3CN}$ was added dropwise with continuous stirring. The color became darker brown, and a black insoluble material separated. The mixture was stirred for further 2 h and then filtered. The black residue was discarded. Upon addition of $\mathrm{Et_2O}$ (50 mL) to the filtrate, a microcrystalline material deposited. It was isolated by filtration, washed with MeOH and $\mathrm{Et_2O}$, and dried *in vacuo* (yield 0.04 g, 36%). Electronic spectrum ($\mathrm{CH_3CN}$): $\lambda_{\max}$ (ϵ_M) 525 (9600), 440 (9800), 240 (45 000) nm. Anal. Calcd for $\mathrm{Mo_2Fe_6S_4Cl_4C_{45}H_{100}N_6O_8}$ (**6**, MW 1809.06): C, 29.85; H, 5.53; N, 4.64. Found: C, 29.46; H, 5.45; N, 4.48. Far-infrared spectrum: 328 (sh), 336 (vs), 360 (m), 409 (s) and 470 (w) $\mathrm{cm^{-1}}$. Mid-infrared spectrum: $\nu(\mathrm{C{\equiv}N})$ 2137 (w) $\mathrm{cm^{-1}}$, $\nu_{\mathrm{asym}}(\mathrm{C{=}O})$ 1648 (s), 1675 (vs), 1700 (s) $\mathrm{cm^{-1}}$, $\nu_{\mathrm{sym}}(\mathrm{C{-}O})$ 1364 (s) $\mathrm{cm^{-1}}$.

Method B. An amount of **4** (0.40 g, 0.40 mmol) was dissolved in 30 mL of $\mathrm{CH_3CN}$, and a solution of $(\mathrm{Et_4N})\mathrm{CN}$ (0.03 g, 0.20 mmol) in 5 mL of $\mathrm{CH_3CN}$ was added dropwise via a pressure-equalizing funnel over 0.5 h. As the solution was stirred for three additional hours, the color became darker brown. To this brown solution, a solution of $(\mathrm{Et_4N})\mathrm{SH}$ (0.06 g, 0.33 mmol) in 5 mL of $\mathrm{CH_3CN}$ was dropwise. After 2 h of stirring the mixture was filtered to remove a black insoluble byproduct and $\mathrm{Et_2O}$ (60 mL) was added to the dark-brown filtrate. A powdery material precipitated and was isolated by filtration and washed with MeOH and $\mathrm{Et_2O}$. The compound was recrystallized from $\mathrm{CH_3CN/Et_2O}$ to afford a microcrystalline material which was isolated and dried in vacuum (yield 0.11 g, 30%). The spectroscopic features of this product are identical to those of the compound obtained by method A.

$(\mathrm{Et_4N})_3[\mathrm{MoFe_3S_4Cl_3(Hcit)}]$ (7). A solution of **1** (1.00 g, 0.96 mmol) in ~40 mL of $\mathrm{CH_3CN}$ was treated with $(\mathrm{Et_4N})$(citrate) (0.45 g, 1.44 g, 1.5-fold excess). The resulting slurry was gently heated to 50 °C and stirred for 12 h. It was then cooled at 25 °C and filtered to remove the excess of $(\mathrm{Et_4N})$(citrate). Upon addition of $\mathrm{Et_2O}$ (100 mL) to the dark-brown filtrate, an oily material precipitated. The clear pale brown supernatant liquid was decanted and the oil was dried *in vacuo* to afford a brown-black powder (yield 0.90 g, 90%), which was washed consecutively with small portions of acetone, methanol, and $\mathrm{Et_2O}$ and was finally recrystallized from $\mathrm{CH_3CN/Et_2O}$ to afford an analytically pure sample. Electronic spectrum ($\mathrm{CH_3CN}$): $\lambda_{\max}$ (ϵ_M) 560 (1070), 470 (1440), 317 (5800) nm. Anal. Calcd for $\mathrm{MoFe_3Cl_3S_4O_7N_3C_{30}H_{65}}$ (**7**, MW 1077.08): C, 33.42; H, 6.03; N, 3.90. Found: C, 33.31; H, 6.00; N, 3.96. Far-infrared spectrum: 242 (w), 278 (w), 303 (m), 319 (m), 338 (sh), 349 (vs), 374 (w), 392 (w), 413 (m) $\mathrm{cm^{-1}}$. Mid-infrared spectrum: $\nu_{\mathrm{asym}}(\mathrm{C{=}O})$ 1604 (vs), 1650 (s), 1720 (m) $\mathrm{cm^{-1}}$; $\nu_{\mathrm{sym}}(\mathrm{C{-}O})$ 1353 $\mathrm{cm^{-1}}$; $\nu(\mathrm{O{-}H})$ 3543 (sh) $\mathrm{cm^{-1}}$.

$(\mathrm{Et_4N})_2[\mathrm{MoFe_3S_4Cl_3(H_2cit)}]$ (8). A solution of **1** (0.20 g, 0.19 mmol in 20 mL of $\mathrm{CH_3CN}$) was treated with anhydrous citric acid (0.037 g, 0.19 mmol). After prolonged stirring at ~50 °C (~12 h), filtration (no residue), and addition of 70 mL of $\mathrm{Et_2O}$ to the dark brown filtrate, a black powder precipitated after overnight standing. It was isolated by filtration, washed consecutively with acetone, EtOH, and $\mathrm{Et_2O}$, and dried *in vacuo* (yield 0.11 g, 60%). Electronic spectrum ($\mathrm{CH_3CN}$): $\lambda_{\max}$ (ϵ_M) 554 (1510), 471 (2020) nm. Anal. Calcd for $\mathrm{MoFe_3Cl_3S_4O_7N_2C_{22}H_{46}\cdot{}^1/_2CH_3CN}$ (**8**, MW 968.13): C, 28.48; H, 4.90; N, 3.61. Found: C, 28.66; H, 5.32; N, 3.92. (Evidence of $\mathrm{CH_3CN}$ of solvation can be seen in the mid-infrared spectrum of the compound: 2249 $\mathrm{cm^{-1}}$ (w)). Far-infrared spectrum: 283 (w), 307 (m), 324 (m), 353 (vs), 382 (sh), 394 (sh), 414 (m) $\mathrm{cm^{-1}}$. Mid-infrared spectrum: $\nu_{\mathrm{asym}}(\mathrm{C{=}O})$ 1592 (vs), 1651 (vs), 1723 (vs) $\mathrm{cm^{-1}}$; $\nu_{\mathrm{sym}}(\mathrm{C{-}O})$ 1394 $\mathrm{cm^{-1}}$; $\nu(\mathrm{O{-}H})$ 3570 (sh, br) $\mathrm{cm^{-1}}$.

$(\mathrm{Et_4N})_2[\mathrm{MoFe_3S_4Cl_3(Hcmal)}]$ (9). A solution of **1** was prepared (0.30 g, 0.29 mmol) in $\mathrm{CH_3CN}$, and an amount of (*R*)-(−)-citramalic acid (0.075 g, 0.44 mmol, 1.5-fold excess) was added to it as a solid. The mixture was heated to 50 °C and vigorously stirred for 24 h. At this point it was allowed to cool at room temperature and then filtered to remove the excess acid. Upon addition of 70 mL of $\mathrm{Et_2O}$ to the dark brown filtrate, an oily material precipitated which was recrystallized from $\mathrm{CH_3CN/Et_2O}$ to afford a brown-black powder. It was washed with MeOH, acetone, and $\mathrm{Et_2O}$ and dried in vacuum (yield 0.16 g, 65%). Electronic spectrum ($\mathrm{CH_3CN}$): $\lambda_{\max}$ (ϵ_M) 465 (3400), 315 (11 300) nm. Anal. Calcd for $\mathrm{MoFe_3Cl_3S_4O_5N_2C_{21}H_{46}\cdot{}^1/_2CH_3CN}$ (**9**, MW 924.13): C, 28.56; H, 5.14; N, 3.79. Found: C, 28.18; H, 5.27; N, 3.86. Far infrared spectrum: 282 (w), 327 (m), 355 (vs), 384 (w), 394 (w), 414 (m) $\mathrm{cm^{-1}}$. Mid-infrared spectrum: $\nu_{\mathrm{asym}}(\mathrm{C{=}O})$ 1590 (vs), 1650 (vs) $\mathrm{cm^{-1}}$; $\nu_{\mathrm{sym}}(\mathrm{C{-}O})$ 1393 $\mathrm{cm^{-1}}$; $\nu(\mathrm{O{-}H})$ 3580 (sh, br) $\mathrm{cm^{-1}}$.

$(\mathrm{Et_4N})_2[\mathrm{MoFe_3S_4Cl_3(Hmal)}]$ (10). An amount of **1** (0.30 g, 0.29 mmol) was dissolved in 30 mL of $\mathrm{CH_3CN}$ and was allowed to react with D-malic acid (58 mg, 0.44 mmol, 1.5-fold excess). The mixture was vigorously stirred and gently heated (~50 °C) for 24 h. At that point the color had become darker brown. The flask was allowed to cool at room temperature, and the mixture was filtered to remove the excess of the acid. Upon addition of $\mathrm{Et_2O}$ (50 mL) to the filtrate a dark brown oil precipitated. The supernatant liquid was decanted and the oil was dried *in vacuo* to afford a brown-black powder. It was washed consecutively with EtOH, acetone, and $\mathrm{Et_2O}$ and was recrystallized from $\mathrm{CH_3CN/Et_2O}$ to afford a brown-black powder (yield 0.15 g, 60%). Electronic spectrum ($\mathrm{CH_3CN}$): $\lambda_{\max}$ (ϵ_M) 460 (3300), 319 (11 500). Anal. Calcd for $\mathrm{MoFe_3Cl_3S_4O_5N_2C_{20}H_{44}}$ (**10**, MW 890.08): C, 26.96 H, 4.94; N, 3.15. Found: C, 26.77; H, 4.32; N, 2.99. Far-infrared spectrum: 303 (w), 318 (w), 347 (vs), 358 (vs), 383 (w), 396 (w), 414 (m) $\mathrm{cm^{-1}}$. Mid-infrared spectrum: $\nu_{\mathrm{asym}}(\mathrm{C{=}O})$ 1630 (s), 1670 (vs) $\mathrm{cm^{-1}}$; $\nu_{\mathrm{sym}}(\mathrm{C{-}O})$ 1392 $\mathrm{cm^{-1}}$; $\nu(\mathrm{O{-}H})$ 3585 $\mathrm{cm^{-1}}$.

$(\mathrm{Et_4N})_2[\mathrm{MoFe_3S_4Cl_3(mida)}]$ (11). An amount of **1** (0.40 g, 0.38 mmol) was dissolved in 30 mL of $\mathrm{CH_3CN}$. A solution of (methylimino)diacetic acid was prepared in MeOH (0.06 g, 0.38 mmol in 5 mL of MeOH) and was added dropwise to the solution of **1** under vigorous stirring. The mixture was stirred overnight at slightly elevated temperature (~50 °C) and then filtered to remove a small amount of black residue. $\mathrm{Et_2O}$ (~50 mL) was layered onto the dark brown filtrate, and after standing for several hours, a microcrystalline solid precipitated. It was isolated by filtration, washed consecutively with MeOH, acetone, and $\mathrm{Et_2O}$, and finally recrystallized from $\mathrm{CH_3CN/Et_2O}$ to afford a crystalline solid as black needles (yield 0.15 g, 43%). Electronic spectrum ($\mathrm{CH_3CN}$): $\lambda_{\max}$ (ϵ_M) 550 (900), 316 (4600). Anal. Calcd

Table 1. Summary of Crystal Data, Intensity Collection, and Structure Refinement Parameters for **3**−**6** and **11**

	3	**4**	**5**	**6**	**11**
formula	$Mo_2Fe_6Cl_8S_8O_4N_4C_{34}H_{80}$	$MoFe_3Cl_4S_4O_4N_3C_{26}H_{60}$	$MoFe_3Cl_3S_4O_4N_4C_{27}H_{60}$	$Mo_2Fe_6Cl_4S_9O_8N_6C_{45}H_{100}$	$MoFe_3Cl_3S_4O_4N_3C_{21}H_{47}$
mol wt	1676.11	1011.53	1002.08	1809.06	903.79
a (Å)	29.70(1)	10.379(3)	10.331(2)	15.125(4)	10.356(3)
b (Å)	12.462(3)	22.682(8)	22.580(6)	21.254(7)	11.506(4)
c (Å)	19.477(4)	18.735(7)	19.083(4)	23.40(1)	15.474(7)
α (deg)					98.14(3)
β (deg)	155.76(2)	92.21(1)	91.97(2)	94.62(3)	100.64(3)
γ (deg)					92.02(3)
V (Å^3)	6492(3)	4407(2)	4449(2)	7512(8)	1790(1)
Z	4	4	4	4	2
cryst system	monoclinic	monoclinic	monoclinic	monoclinic	triclinic
space group	$C2/c$	$P2_1/n$	$P2_1/n$	$P2_1/n$	$P\bar{1}$
cryst size (mm)	0.18 × 0.05 × 0.45	0.58 × 0.30 × 0.15	0.60 × 0.30 × 0.24	0.30 × 0.40 × 0.32	0.30 × 0.12 × 0.43
d_{calcd} (g/cm^3)	1.72	1.53	1.48	1.67	1.68
d_{obsd} (g/cm^3)^{a,b}	1.72^a	1.53^b	1.50^b	1.64^a	1.69^a
radiation (λ (Å))	Mo Kα (0.710 73)	Mo Kα (0.710 73)	Mo Kα (0.710 73)	Mo Kα (0.710 73)	Mo Kα (0.710 73)
abs coeff μ (cm^{-1})	22.83	16.20	16.2	19.5	20.1
scan speed (deg/min)	1.00−5.00	1.50−15.00	1.50−15.00	1.50−15.00	1.50−15.00
scan range (deg)	$1.8 + (2\theta_{K\alpha 1} - 2\theta_{K\alpha 2})$	$1.2 + (2\theta_{K\alpha 1} - 2\theta_{K\alpha 2})$	$1.2 + (2\theta_{K\alpha 1} - 2\theta_{K\alpha 2})$	$1.2 + (2\theta_{K\alpha 1} - 2\theta_{K\alpha 2})$	$1.2 + (2\theta_{K\alpha 1} - 2\theta_{K\alpha 2})$
bkgd/scan time ratio	0.5	0.5	0.5	0.5	0.5
data collcd (deg) (octants)	5−45 ($+h,+k,\pm l$)	3−45 ($+h,+k,\pm l$)	3−45 ($+h,+k,\pm l$)	4−40 ($+h,+k,\pm l$)	3−45 ($\pm h,\pm k,\pm l$)
tot. reflcns	5446	6160	5480	7620	9740
unique data	3943	5789	5079	7003	9422
refined reflcns	2719	3617	3303	3557	3494
no. of variables (data/param ratio)	318 (8.6)	406 (8.9)	415 (7.9)	511 (7.0)	352 (9.9)
goodness of fit	1.43	1.87	2.78	3.20	1.72
R (%)^d	6.22	4.35	5.41	8.73	5.14
R_w (%)^e	5.68^f	4.39^g	4.87^g	9.42^h	5.41^i

[a] By flotation in dibromoethane/CCl_4 mixture. [b] By flotation in CCl_4/hexane mixture. [c] At ambient temperature. [d] $R = \sum(|F_o - F_c|)/\sum|F_o|$. [e] $R_w = [\sum(w|F_o - F_c|)^2/\sum w(F_o)^2]^{1/2}$. [f] $w^{-1} = \sigma^2(F_o) + 0.000368(F_o)^2$. [g] $w^{-1} = \sigma^2(F_o) + 0.001(F_o)^2$. [h] $w^{-1} = \sigma^2(F_o) + 0.002415(F_o)^2$. [i] $w^{-1} = \sigma^2(F_o) + 0.001(F_o)^2$.

for $MoFe_3S_4Cl_3O_4N_3C_{21}H_{47}$ (**11**, MW 903.72): C, 27.88; H, 5.20; N, 4.65. Found: C, 27.78; H, 5.07; N, 4.74. Far-infrared spectrum: 287 (w), 302 (w), 328 (vs), 357 (vs), 396 (w), 413 (s), 471 (m) cm^{-1}. Mid-infrared spectrum: ν_{asym}(C=O) 1645 (vs), 1671 (vs) cm^{-1}; ν_{sym}(C−O) 1396 (s) cm^{-1}.

Oxidation of $(Et_4N)_4\{(MoFe_3S_4Cl_4)_2(\mu\text{-}C_2O_4)\}$ with Ferrocenium Hexafluorophosphate. A solution of **3** (0.40 g, 0.24 mmol in 20 mL of DMF) was treated with a solution of $FcPF_6$ (0.14 g, 0.48 mmol in 5 mL of DMF). The reaction vessel was slightly evacuated, and the contents were vigorously stirred for ~20 h. During that time the solution had turned from dark brown to brown-orange. The solution was filtered to remove a small amount of black insoluble material, and Et_2O (70 mL) was slowly added to the filtrate. After overnight standing, brown-orange needles deposited on the walls of the flask. They were isolated by filtration and washed with Et_2O (yield 0.2 g, 60%). The identify of this material was confirmed by its characteristic spectroscopic features as the $(Et_4N)_2(Cl_2FeS_2MoS_2FeCl_2)$ linear trimer.[26] Electronic spectrum (CH_3CN): λ_{max} (ϵ_M) 600 (sh), 522 (sh), 472 (5850), 432 (4070), 314 (12 250) nm. Far-infrared spectrum: 324 (vs), 344 (m), 351 (m), 382 (s), 412 (w) cm^{-1}.

Reaction of $(Et_4N)_4\{[MoFe_3S_4Cl_4]_2(\mu\text{-}C_2O_4)\}$ with Tetrachloro-1,2-benzosemiquinone. An amount of **3** (0.30 g, 0.18 mmol) was dissolved in 30 mL of CH_3CN, tetrachloro-1,2-benzoquinone (0.044 g, 0.09 mmol) and tetrachlorocatechol (0.044 g, 0.09 mmol, deprotonated with Et_4NOH) were mixed in CH_3CN, and the resulting orange-red solution was slowly added to the dark brown cluster solution. A brown-orange color started to develop. The flask was evacuated and stirred overnight. The mixture was then filtered to remove a small amount of black residue, and upon slow addition of Et_2O (80 mL) to the filtrate, a microcrystalline material deposited after standing for 6 h. Recrystallization from CH_3CN/Et_2O afforded black crystals (yield 0.18 g, 60%). This material was identical in electronic and mid- and far-infrared spectra to those of $(Et_4N)_2[MoFe_3S_4Cl_3(Cl_4\text{-cat})(CH_3CN)]$, **1**.[25]

X-ray Structural Determinations. For all structure determinations reported herein, single crystals suitable for diffraction experiments were obtained by vapor diffusion of Et_2O into CH_3CN solutions of the compounds. The crystals were mounted with Apiezon grease in quartz capillaries (Charles Supper Co.) under argon atmosphere, and the capillaries were then flame sealed. Crystal data, intensity collection information, and structure refinement parameters for all structures are provided in Table 1. Diffraction experiments were conducted at ~25 °C on either a Syntex P2₁m/v (compound **3**) or a Nicolet P3F (compounds **4**−**6** and **11**) four-circle computer-controlled diffractometer using graphite-monochromatized ($2\theta_m$ = 12.50°) Mo Kα radiation (λ = 0.710 73 Å). Intensity data were collected by using a $\theta - 2\theta$ step scan technique.[27] The raw data were reduced to net intensities, and appropriate corrections were applied to the data according to previously described protocols.[27] Computer programs were those of the SHELXTL structure determination package (Nicolet XRD Corp., Fremont, CA).

Solution and Refinement of the Structures. The direct methods routine SOLV of the SHELXTL 88 package of the crystallographic program was used to solve the structures. The solutions were verified in Patterson synthesis maps. Trial positions of Mo, Fe, and core S atoms were taken from the *E*-map derived from the unique phase set with the next-to-highest combined figure of merit. The remaining non-hydrogen atoms were located by subsequence difference Fourier maps. In all structures and in the final stages of refinement the hydrogen atoms were included in the structure factor calculations at fixed positions (C−H bond length of 0.96 Å) with thermal parameters set to 1.2× those of the appropriate C atoms.

---

(26) (a) Coucouvanis, D.; Simhon, E. D.; Stremple, P. P.; Ryan, M.; Swenson, D.; Baenziger, N. C.; Simopoulos, A.; Papaefthymiou, V.; Kostikas, A.; Petrouleas, V. *Inorg. Chem.* **1984**, *23*, 741. (b) Coucouvanis, D.; Baenziger, N. C.; Simhon, E. D.; Stremple, P. P.; Swenson, D.; Simopoulos, A.; Kostikas, A.; Petrouleas, V.; Papaefthymiou, V. *J. Am. Chem. Soc.* **1980**, *102*, 1732.

(27) Baenziger, N. C.; Foster, B. A.; Howells, M.; Howells, R.; Vander Valk, P.; Burton, D. J. *Acta Crystallogr., Sect. B* **1977**, *B33*, 2327.

(a) $(Et_4N)_4[MoFe_3S_4Cl_4)_2(\mu\text{-}C_2O_4)$ (3). The structure was refined by the block-cascade least-squares method. All Mo, Fe, S, Cl, O, and C atoms of the anion were refined anisotropically. The remaining atoms had isotropic temperature coefficients. The tetraanion is located on a crystallographic inversion center in the lattice. There are 16 Et_4N^+ cations in the lattice, 8 of which occupy general positions, 4 sit on crystallographic mirror planes, and 4 occupy an inversion center. The cations on the inversion center were disordered, and this disorder was modeled by refining the methyl carbons at full occupancy, while the carbons bonded to the N were placed in two alternate positions at 50% occupancy.

(b) $(Et_4N)_3[MoFe_3S_4Cl_4(C_2O_4)]$ (4). The structure was refined by the full-matrix least-squares method. All the atoms in the anion were refined with anisotropic thermal parameters. The asymmetric unit consists of a complete anion and three complete Et_4N^+ cations which do not show any disorder.

(c) $(Et_4N)_3[MoFe_3S_4Cl_3(C_2O_4)(CN)]$ (5). All the atoms of the anion and the three cations (except the H's) were refined with anisotropic thermal parameters. One complete anion and three complete Et_4N^+ cations were found to be located in the asymmetric unit. No disorder problems were identified in the Et_4N^+ cations.

(d) $(Et_4N)_5\{[MoFe_3S_4Cl_2(C_2O_4)]_2(\mu\text{-}S)(\mu\text{-}CN)\}$ (6). All the atoms in the pentaanion (except the C of the cyanide and one C of the oxalate) were refined anisotropically as well as the N atoms of the cations. The C atoms of the cations were isotropically refined. The asymmetric unit consists of a complete pentaanion and five complete Et_4N^+ cations, which do not exhibit any kind of disorder.

(e) $(Et_4N)_2[MoFe_3S_4Cl_3(\text{mida})]$ (11). All the atoms of the anion and the Et_4N^+ cations were refined anisotropically. The asymmetric unit consists of a complete dianion and two complete Et_4N^+ cations, which do not exhibit any kind of disorder. In the final stages of refinement, the hydrogen atoms (C−H bond length 0.96 Å) were included in the structure factor calculations but were not refined.

Crystallographic Results. Selected intramolecular distances and angles for the anions in **3**−**6** and **11** with standard deviations derived from the inverse matrices of the least-squares refinements are included in Tables 5−8. The final atomic positional and thermal parameters for cluster **11** with standard deviations derived from the inverse matrix of the final least-squares refinement have been deposited as supplementary material. The labeling schemes are shown in Figures 2−5.

Results and Discussion

Synthesis. The single cubane $[MoFe_3S_4Cl_3(Cl_4\text{-cat})(CH_3CN)]^{2-}$, **1**, is readily synthesized from its double cubane precursor $[Mo_2Fe_6S_8(SEt)_6(Cl_4\text{-cat})_2]^{4-}$, **2**, upon addition of a stoichiometric amount of PhCOCl, with the concomitant elimination of PhCOSEt. This and similar clusters have been extensively used as starting materials principally in substitution reactions on the labile Mo site, yielding a number of clusters with Mo-bound nitrogenase pseudosubstrates.[20b,c,d,21g,28] To our knowledge, substitution of the catecholate ligand in the $MoFe_3S_4$ cubanes, by ligands different than other catecholates,[20d] has not been reported previously. The reaction of **1** with anhydrous oxalic acid results in protonation of the Mo-bound Cl_4-cat. The oxalate dianion is found incorporated within the double cubane end product, **3**, as a μ_2-η^4 bridge between the two Mo atoms. Although the Cl_4-cat:oxalic acid stoichiometry used in the reaction is 1:1, only one oxalate ligand is found per two cubanes in the final product in what appears to be an "all or nothing" reaction. This dimerization undoubtedly is due to the pronounced tendency of the oxalate ligand to form dimeric structures.[29] The same reaction when attempted with 0.5 equiv of oxalic acid per cubane unit also afforded **3**, in somewhat lower yields.[30] When excess oxalic acid was used, cluster decomposition occurred and very low yields of the final product were obtained. The presence of the Cl^- ligand on the Mo atom in **3**, revealed by X-ray crystallography (*vide infra*), is somewhat intriguing considering that, initially, *no external source of Cl^- was supplied.* It appears that the Cl^- ions are supplied by the partial decomposition of the cluster. As a result the yields of **3** never exceed 70% in the absence of an external source of Cl^-. The addition of a stoichiometric amount of Et_4NCl in the synthetic procedure resulted in nearly quantitative yields of **3**. At present it is not clear why the $MoFe_3S_4$ cubanes with Mo-bound oxalate ligands readily bind Cl^-, whereas **1** does not, even when Cl^- is present in large excess.[20e] The double cubane structure of **3** is ruptured when treated with a soluble source of oxalate ($(Et_4N)_2(C_2O_4)$) and gives **4**. This process affords optimum yields (55%) when a dilute solution of $(Et_4N)_2(C_2O_4)$ is added to a concentrated solution of **3**. The optimum time period for the synthesis of **4** was found to be 2−3 h. Upon prolonged stirring of this reaction mixture (>12 h), gradual cluster degradation occurs and decomposition products are obtained with infrared spectra suggestive of Fe−thiomolybdate complexes with a Mo−oxo moiety (M−S−M, ~470 cm^{-1}, and Mo=O, ~920 cm^{-1}). The Cl^- ligand in **4** is readily substituted by CN^- (supplied as $(Et_4N)CN$) and affords the cyano-derivative cluster, **5**, in nearly quantitative yield. There is no apparent evidence of CN^- attack on the Fe sites, and multiple C−N vibrational frequencies are not observed in the infrared spectra of the compound. The reaction of **4** with 0.5 equiv of $(Et_4N)CN$ followed by sulfide coupling with $(Et_4N)SH$ leads to the formation of the doubly-bridged double cubane **6** in moderate purified yields (30%). Such sulfide coupling reactions have been well established by the effective formation of clusters analogous to **6**.[21f,g,31,32] The sulfide coupling reactions do not give satisfactory results with either Li_2S or Na_2S and lead to complete decomposition of the cluster. The insolubility of the Li^+ or Na^+ salts of the $C_2O_4{}^{2-}$ anion in CH_3CN solution and precipitation of $Li_2C_2O_4$ or $Na_2C_2O_4$ may be a driving force for this cluster decomposition reaction. Alternative routes to Mo-bound oxalate doubly-bridged double cubanes, DBDC, of the general type $\{[MoFe_3S_4Cl_2(C_2O_4)]_2(\mu\text{-}S)(\mu\text{-}X)\}^{n-}$ (X = intercluster bridging ligand) were sought by reacting the double cubanes $\{[MoFe_3S_4Cl_2(Cl_4\text{-cat})]_2(\mu\text{-}S)(\mu\text{-}X)\}^{n-}$ [19b] (X = NH_2-NH_2, $n = 4$; X = OH^-, $n = 5$; X = CN^-, $n = 5$; X = S^{2-}, $n = 6$) with oxalic acid. The only isolable product in low yields was **3** which was identified by its characteristic spectral features. Apparently protonation of both S^{2-} and X bridges in the DBDC clusters leads to decomposition.

The reactions of **1** with hydroxy−polycarboxylic acids of the general type $HOOCCH_2C(R)(OH)(COOH)$ (R = H, D-malic; R = CH_3, *R*-citramalic; R = CH_2COOH, citric) or (methylimino)diacetic acid proceed with protonation of the catecholate ligand and formation of the polycarboxylate cluster derivatives that contain a Mo-bound tridentate polycarboxylate ligand. The reaction of **1** with malonic acid $HOOCCH_2COOH$, which is of comparable acidity to e.g. citric acid,[33] did not take place to any significant extent, and the solid isolated at the end of the

---

(28) Mosier, P. E.; Kim, C. G.; Coucouvanis, D. *Inorg. Chem.* **1993**, *32*, 3620.

(29) (a) Oldham, C. In *Comprehensive Coordination Chemistry*; Wilkinson, G., Gillard, R. D., McCleverty, J. A., Eds.; Pergamon Press: New York, 1984; Vol. 2, p 435. (b) Darensbourg, D. J.; Chojnacki, J. A.; Reibenspeis, J. H. *Inorg. Chem.* **1992**, *31*, 3428. (c) Cortés, R.; Urtiaga, M. K.; Lezama, L.; Arriortua, M. I.; Rojo, T. *Inorg. Chem.* **1994**, *33*, 829.

(30) The possibility of the requirement of only one proton for the complete dissociation of the Cl_4-cat ligand (apparently as Cl_4-catH$^-$) cannot be excluded at this point. Our attempts to isolate and characterize possible byproducts of this reaction did not have any success.

(31) Challen, P. R. Ph.D. Thesis, The University of Michigan, 1990.

(32) Challen, P. R.; Koo, S. M.; Dunham, W. R.; Coucouvanis, D. *J. Am. Chem. Soc.* **1990**, *112*, 2455.

reaction (after 3 days at 50 °C) showed only a weak C=O vibration at ~1640 cm^{-1}.

Vibrational Spectra. (a) The 140–500 cm^{-1} Region. The spectra of all the Mo/Fe/S clusters show a variety of features in this region. A prominent band in the 330–360 cm^{-1} region displays sufficient variety of patterns for the different clusters that makes it useful as a diagnostic tool. This band often appears as a doublet or multiplet depending on the symmetry of the cubane unit. It is principally assigned to Mo–μ_3-S, Fe–μ_3-S, and Fe–Cl skeletal vibrations or a combination of them.[31,34]

(b) The 400–4000 cm^{-1} Region. Formation of all the Mo-bound carboxylate $MoFe_3S_4$ clusters is manifested by dramatic changes in the vibrational spectrum of the starting compound **1**. Briefly, we point out some of its spectral features which are subject to changes. The Mo-coordinated CH_3CN ligand gives rise to a weak doublet at 2284 and 2312 cm^{-1}, consistent with various transition metal acetonitrile complexes.[35] The Cl_4-cat ligand gives rise to a strong band at ~1255 cm^{-1} assigned to the C–O stretch.[36] The region 1300–1500 cm^{-1} appears complicated due to strong C–C absorptions from the Et_4N^+ cations. Nevertheless, a strong band at 1430 cm^{-1} is tentatively assigned to C–C aromatic stretches from the Cl_4-cat ring.[36a,d,e] A medium-intensity vibration at 542 cm^{-1} is assigned to the Mo–O(Cl_4-cat) stretch and agrees well with values reported in the literature.[36b] The most profound change in the vibrational spectrum of **1** upon its reaction with carboxylic acids is the appearance of intense absorptions due to C=O stretches in the 1590–1720 cm^{-1} region. In all cases the peaks assigned to the Mo–(Cl_4-cat) moiety vanish in the final product and their absence is considered evidence for purity. In **3** the most intense asymmetric C=O vibration is found at 1635 cm^{-1} and the symmetric one at 1460 cm^{-1}. This gives rise to a $\Delta\nu$ (ν_{asym}(C=O) − ν_{sym}(C–O)) of 175 cm^{-1} characteristic of a bridging tetradentate oxalate ligand.[37] In **4** the ν_{asym}(C=O) shifts to 1670 cm^{-1} and the ν_{sym}(C–O) to 1378 cm^{-1}, with Δ = 289 cm^{-1}, typical for terminal bidentate oxalate.[38] The ν_{asym}(C=O) and ν_{sym}(C–O) in **5** and **6** show insignificant changes compared to the parent **4**. Compound **5** displays a weak sharp stretch at 2123 cm^{-1} assigned to the terminally bound CN^-,[39] whereas in **6** the bridging nature of the CN^- gives rise to a hypsochromically shifted weak vibration at 2136 cm^{-1}.[39]

Table 2. Vibrational Spectroscopy Data for Compounds **3**–**11**

compd	ν_{asym}(C=O) (cm^{-1})	ν_{sym}(C–O) (cm^{-1})	Δ (cm^{-1})
3	1635 (vs) 1667 (m) 1695 (w)	1460 (s)	175
4	1637 (m) 1667 (vs) 1698 (w)	1378 (m)	289
5	1639 (m) 1672 (vs) 1700 (s)	1378 (s)	294
6	1648 (sh) 1675 (vs) 1700 (m)	1364 (s)	311
7	1604 (vs) 1650 (vs) 1720 (m)	1354 (s)	296
8	1592 (vs) 1651 (vs) 1723 (s)	1394 (s)	257
9	1590 (vs) 1650 (vs)	1393 (s)	257
10	1630 (s) 1670 (vs)	1392 (s)	278
11	1645 (vs) 1671 (vs)	1396 (s)	275

In the hydroxy–polycarboxylate cubanes, the spectra are more complicated. Cluster **7** displays three strong asymmetric C=O vibrations at 1604, 1650, and 1720 cm^{-1}, whereas one symmetric vibration is found at 1354 cm^{-1}. The malate and citramalate analogs display stretches at 1630, 1670 and 1590, 1650 cm^{-1}, respectively. It should be noted that clusters **7** and **8** show a vibration at 1720 and 1723 cm^{-1}, respectively, which arises from a protonated, uncoordinated carboxylate moiety (–COOH).[40] This vibration is absent from **9**–**11** which lack such a group and presumably have all their carboxylate groups coordinated to the Mo. A weak broad stretch at 3543 cm^{-1} in **7** is tentatively assigned to the hydroxyl group of the free –COOH and can be detected only in highly crystalline samples. A set of peaks at 500, 540, and 563 cm^{-1} are tentatively assigned to a Mo–O(alkoxide) group. Vibrations in this region have been detected for many transition metal alkoxides.[41] Cluster **11** displays strong vibrations at 1645, 1671, and 1396 cm^{-1}, assigned to the ν_{asym}(C=O) and ν_{sym}(C–O) stretches, respectively.[42a,b] The results from the vibrational spectroscopic studies are tabulated in Table 2.

Electronic Spectra. The electronic spectrum of $[(MoFe_3S_4Cl_4)_2(\mu\text{-}C_2O_4)]^{4-}$, **4** (Table 3), is without prominent features in the visible region and consists of a steadily rising absorbance from 750 nm into the UV region with slight shoulders at 570 and 475 nm. A similar situation prevails for the clusters **7**–**11**. Generally, the electronic spectra of these clusters are of little diagnostic value due to the lack of well-defined, intense absorptions.

Electrochemical Measurements. The only other single cubane cluster $[MoFe_3S_4]^{3+}$, with Fe-bound terminal chloride

---

(33) Comparative data are available in DMF solvent: Izutsu, K. *Acid-Base Dissociation Constants in Dipolar Aprotic Solvents*; IUPAC Chemical Data Series, No. 35; Blackwell Scientific Publications: Oxford, U.K., 1990; pp 39–63.

(34) (a) Nakamoto, K. *Infrared and Raman Spectra of Inorganic and Coordination Compounds*; Wiley-Interscience: New York, 1986; p 411. (b) Czernuszewicz, R. S.; Macor, K. A.; Johnson, M. K.; Gerwirth, A.; Spiro, T. G. *J. Am. Chem. Soc.* **1987**, *109*, 7178.

(35) Storhoff, B. N.; Lewis, H. C., Jr. *Coord. Chem. Rev.* **1977**, *23*, 1.

(36) (a) Wicklund, P. A.; Brown, D. G. *Inorg. Chem.* **1976**, *15*, 396. (b) Nielson, A. J.; Griffith, W. P. *J. Chem. Soc., Dalton Trans.* **1978**, 1501. (c) Sofen, S. R.; Ware, D. C.; Cooper, S. R.; Raymond, K. N. *Inorg. Chem.* **1979**, *18*, 234. (d) Griffith, W. P.; Pumphrey, C. A.; Rainey, T. A. *J. Chem. Soc., Dalton Trans.* **1986**, 1125. (e) Edwards, C. F.; Griffith, W. P.; White, A. J. P.; Williams, D. J. *J. Chem. Soc., Dalton Trans.* **1992**, 957.

(37) (a) Curtis, N. F. *J. Chem. Soc. A* **1968**, 1584. (b) Nomoyama, K.; Ojima, H.; Ohki, K.; Nomoyama, M. *Inorg. Chim. Acta* **1980**, *41*, 155. (c) Bencini, A.; Benelli, C.; Gatteschi, D.; Zanchini, C.; Fabretti, A. C.; Franchini, G. C. *Inorg. Chim. Acta* **1984**, *86*, 169. (d) Castro, I.; Faus, J.; Julve, M.; Mollar, M.; Monge, A.; Gutierrez-Puebla, E. *Inorg. Chim. Acta* **1989**, *161*, 97. (e) Brisdon, B. J.; Hodson, A. G. W.; Mahon, M. F.; Molloy, K. C. *J. Chem. Soc., Dalton Trans.* **1993**, 245.

(38) (a) Fujita, J.; Martell, A. E.; Nakamoto, K. *J. Chem. Phys.* **1962**, *36*, 324. (b) Schmelz, M. J.; Miyazawa, S. I.; Lane, T. J.; Quagliano, J. V. *Spectrochim. Acta* **1957**, *9*, 51. (c) Edwards, H. G. M.; Hardman, P. H. *J. Mol. Struct.* **1992**, *273*, 73. (d) Gleizes, A.; Julve, M.; Verdaguer, M.; Real, J. A.; Faus, J.; Solans, X. *J. Chem. Soc., Dalton Trans.* **1992**, 3209.

(39) (a) Griffith, W. P. *Coord. Chem. Rev.* **1975**, *17*, 177. (b) Golub, A. M.; Kohler, H.; Skopenko, V. V. *Chemistry of the Pseudohalides*; Elsevier: Amsterdam, 1986; p 77.

(40) (a) Glusker, J. P. *Acc. Chem. Res.* **1980**, *13*, 345. (b) Pedrosa de Jesus, J. D. In *Comprehensive Coordination Chemistry*; Wilkinson, G., Gillard, R. D., McCleverty, J. A., Eds.; Pergamon Press: New York, 1984; Vol. 2, p 461. (c) Knobler, C. B.; Wilson, A. J.; Hider, R. N.; Jensen, I.; Penfold, B. R.; Robinson, W. T.; Wilkins, C. J. *J. Chem. Soc., Dalton Trans.* **1993**, 1299.

(41) Bradley, D. C.; Mehrotra, R. C.; Gaur, D. P. *Metal Alkoxides*; Academic Press: London, 1978; p 116.

(42) (a) Appleton, T. G.; Berry, R. D.; Hall, J. R. *Inorg. Chem.* **1985**, *24*, 666. (b) Hoeschele, J. D.; Farrel, N.; Turner, W. R.; Rithner, C. D. *Inorg. Chem.* **1988**, *27*, 4106. (c) Butcher, R. J.; Penfold, B. R. *J. Cryst. Mol. Struct.* **1976**, *6*, 13.

Table 3. Electronic Spectral Data for Various MoFe$_3$S$_4$$-$Carboxylate Clusters, in CH$_3$CN

compd	λ_{max}, nm (ϵ_M)
3	570 (3080), 475 (5250)
4	450 (6420), 310 (13 600)
5	420 (2300), 320 (5400), 240 (14 100)
6	525 (9600), 440 (9800), 240 (45 000)
7	560 (1070), 470 (1440), 317 (5800)
8	554 (1500), 470 (2020)
9	465 (3400), 315 (11 300)
10	460 (3300), 319 (11 500)
11	550 (900), 316 (4600)

Table 4. Cyclic Voltammetric Data for the Clusters **1**, **3**$-$**10**, and **11** in Various Solvents[a]

compds	solvent	reductions (mV)	oxidations (mV)
1	ClCH$_2$CH$_2$Cl	$-$940, qr	+300, irr
1	CH$_3$CN	$-$920, qr	+350, irr
3	CH$_2$Cl$_2$	$-$40, qr; $-$890, qr; $-$1100, irr	+500, qr
3	ClCH$_2$CH$_2$Cl	$-$30, qr; $-$900, irr; $-$1070, irr	+500, qr
3	CH$_3$CN	$-$930, irr; $-$1300, irr	+550, irr
3	DMF	$-$960, irr; 1130, irr	
4	CH$_3$CN	$-$1000, qr	+250, irr
4	CH$_2$Cl$_2$	$-$1040, qr	+200, irr +500, qr
5	CH$_2$Cl$_2$	$-$1090, qr	+350, irr
6	CH$_2$Cl$_2$	$-$30, qr; $-$1110, irr; $-$1500, irr	+300, irr
7	ClCH$_2$CH$_2$Cl	$-$1050, qr	+260, qr
7	DMF	$-$1120, qr	+280, irr
7	CH$_3$CN	$-$1020, qr	+270, irr
8	CH$_2$Cl$_2$	$-$1130, irr	+550, irr
8	CH$_3$CN	$-$1100, irr	+480, irr
9	ClCH$_2$CH$_2$Cl	$-$880, irr	+630, irr
10	CH$_2$Cl$_2$	$-$970, irr	+600, irr
10	CH$_3$CN	$-$1020, irr	+750, irr
11	CH$_2$Cl$_2$	$-$840, rev	+560, irr
11	CH$_3$CN	$-$830, rev	+490, irr

[a] qr = quasi-reversible, irr = irreversible, rev = reversible.

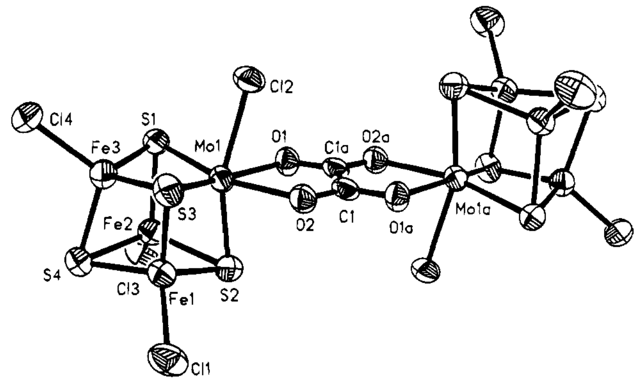

Figure 2. Structure and labeling of [(MoFe$_3$S$_4$Cl$_4$)$_2$(μ-C$_2$O$_4$)]$^{4-}$, anion of **3**. Thermal ellipsoids as drawn by ORTEP represent 40% probability surfaces.

ligands, for which the cyclic voltammetry has been reported is the [(al$_2$-cat)(CH$_3$CN)MoFe$_3$S$_4$Cl$_3$)]$^{2-}$ cluster[20c] (al = allyl). This cluster shows a reversible reduction at $-$1.02 V in CH$_3$CN solution *vs* SCE and a second irreversible reduction at $-$1.84 V. The electrochemical behavior of the single and double cubanes described in this paper was studied in a variety of solvents, and the results are summarized in Table 4. The dominant feature is the multiple reductions exhibited by the oxalate double cubanes. The cyclic voltametric waves are not reversible by electrochemical standards for most of the clusters ($\Delta E \gg 60$ mV). The two reductions of **3** at $-$890 and $-$1100 mV (in CH$_2$Cl$_2$), separated by 210 mV, indicate electronic communication between the two MoFe$_3$S$_4$ subunits through the oxalate bridge. This interaction amounts to ~4.8 kcal mol^{-1} and is found at the weaker side of the range of values found in other bridged cubanes such as [Mo$_2$Fe$_6$S$_8$(SR)$_9$]$^{3-}$ [21b,43] (R = alkyl, aryl), bridged [Fe$_4$S$_4$]$^{2+}$ cores,[32,44] {[(MoFe$_3$S$_4$(S-Ph-p-Cl)$_3$]$_3$(S$_2$)$_2$}$^{4-}$,[45] and heterometal double cubanes with V or Re in the place of Mo.[46] In **6**, two successive irreversible reductions are found at $-$1110 and $-$1500 mV. This difference corresponds to an interaction energy of ~9 kcal mol^{-1} and is consistent with values reported for other doubly-bridged double-cubanes.[21f,g] The doubling of the voltametric waves indicates that the double cubane core of **6** retains its integrity in solution and the entire cluster behaves as an entity with strongly interacting subunits. In accordance with this, **6** is EPR silent. All the single cubanes described herein show single reductions in the 1000$-$1100 mV region. The parent **1** (under identical or similar conditions) displays a reduction at $-$940 mV, a value shifted to more positive potentials, presumably due to the electron-withdrawing effect of the Cl substituents on the catechol, which renders the entire cluster more susceptible to reduction. The cyclic voltammogram of **11** displays a well-defined reversible reduction in CH$_3$CN at $-$830 mV and an irreversible oxidation at +490 mV (corresponding values in CH$_2$Cl$_2$: $-$840 rev, +560 irr).

Description of the Structures. MoFe$_3$S$_4$ Cubane Subunits. The cubane-type [MoFe$_3$(μ_3-S)$_4$]$^{3+}$ cores of the clusters described herein are constructed from the fusion of Fe$_2$S$_2$ and MoFeS$_2$ nonplanar rhombs. Core interatomic distances are within the ranges of corresponding distances in isoelectronic structures;[19,20,21] therefore, they will be *briefly* mentioned here. For more detailed descriptions we refer to excellent reports by Holm *et al.*[20,21a-e] In the present structures the Mo$\cdots$Fe distances range from 2.704(6) to 2.776(6) Å whereas the Fe$\cdots$Fe separations appear to be very similar, with a range from 2.692(3) to 2.755(6) Å.

(Et$_4$N)$_4$[(MoFe$_3$S$_4$Cl$_4$)$_2$(μ-C$_2$O$_4$)] (3). The center of the C$-$C(oxalate) bond in the tetraanionic cluster in **3** (Figure 2) resides on a crystallographic center of symmetry. The Mo$\cdots$Mo separation is found at 5.72 Å, a distance similar to that is reported for other transition metal dimers separated by an oxalate bridge.[37e,47] The Mo atom is located at one corner of the cubane subunit in a distorted octahedral environment as dictated by the angles imposed by the ligand environment (see Table 5). The Cl$^-$ ligands on the Mo atoms are found in a trans arrangement. The Mo$-$Cl bond at 2.500(3) Å is comparable to the one found in [MoFe$_3$S$_4$Cl$_4$(dmpe)],[20e] the only other MoFe$_3$S$_4$ cluster known with a Mo$-$Cl bond. The latter shows a Mo$-$Cl bond length of 2.490(2) Å. Two Mo coordination sites external to the subclusters are occupied by the bridging tetradentate oxalate ligand. Mean Mo$-$O(oxalate) bonds (2.207(7) Å) are longer than the Mo$-$O distances found in the analogous catecholate

---

(43) Christou, G.; Mascharak, P. K.; Armstrong, W. H.; Papaefthymiou, G. C.; Frankel, R. B.; Holm, R. H. *J. Am. Chem. Soc.* **1982**, *104*, 2820.

(44) Stack, T. D. P.; Carney, M. J.; Holm, R. H. *J. Am. Chem. Soc.* **1989**, *111*, 1670.

(45) Kovacs, J. A.; Bashkin, J. K.; Holm, R. H. *Polyhedron* **1987**, *6*, 1445.

(46) (a) Cen, W.; Lee, S. C.; Li, J.; MacDonell, F. M.; Holm, R. H. *J. Am. Chem. Soc.* **1993**, *115*, 9515. (b) Ciurli, S.; Carrie, M.; Holm, R. H. *Inorg. Chem.* **1990**, *29*, 3493. (c) Ciurli, S.; Holm, R. H. *Inorg. Chem.* **1991**, *30*, 743.

(47) (a) Felthouse, T. R.; Laskowski, E. J.; Hendrickson, D. N. *Inorg. Chem.* **1977**, *16*, 1077. (b) Michalowicz, A.; Girerd, J. J.; Goulon, J. *Inorg. Chem.* **1979**, *18*, 3004. (c) Julve, M.; Verdaguer, M.; Gleizes, A.; Levisalles, M. P.; Kahn, O. *Inorg. Chem.* **1984**, *23*, 3808. (d) Ribas, J.; Monfort, M.; Diaz, C.; Solans, X. *Anal. Quim.* **1988**, *84*, 186. (e) Ohba, M.; Tamaki, H.; Matsumoto, N.; Okawa, H. *Inorg. Chem.* **1993**, *32*, 5385.

Table 5. Selected Bond Distances (Å) and Angles (deg) of **3**

	Bond Distances		
Mo1···Mo1a	5.72	Fe1−S4	2.280(3)
Mo1−Fe1	2.719(2)	Fe2−Fe3	2.717(3)
Mo1−Fe2	2.749(2)	Fe2−Cl3	2.216(3)
Mo1−Fe3	2.749(2)	Fe2−S1	2.263(3)
Mo1−Cl2	2.500(3)	Fe3−S2	2.271(3)
Mo1−S1	2.326(2)	Fe2−S4	2.269(4)
Mo1−S2	2.345(3)	Fe3−Cl4	2.211(4)
Mo1−S3	2.327(3)	Fe3−S1	2.269(3)
Mo1−O1	2.196(7)	Fe3−S3	2.276(3)
Mo1−O2	2.218(6)	Fe3−S4	2.272(4)
Fe1−Fe2	2.717(2)	O1−C1a	1.27(1)
Fe1−Fe3	2.734(2)	O1a−C1	1.27(1)
Fe1−Cl1	2.224(2)	O2−C1	1.25(2)
Fe1−S2	2.259(4)	C1−C1a	1.526(9)
Fe1−S3	2.264(4)		
	Angles		
Mo1−S1−Fe2	73.60(8)	S1−Fe3−S4	104.0(1)
Mo1−S1−Fe3	73.49(7)	S2−Mo1−S3	103.4(1)
Mo1−S2−Fe1	72.4(1)	S2−Mo1−O1	84.4(2)
Mo1−S2−Fe2	73.10(9)	S2−Mo1−O2	85.0(2)
Mo1−S3−Fe1	72.6(1)	S2−Fe1−S3	108.2(1)
Mo1−S3−Fe3	73.35(9)	S2−Fe1−S4	103.7(1)
Mo1−O1−Cla	115.1(5)	S2−Fe2−S4	103.7(1)
Mo1−O2−Cl	113.8(4)	S3−Mo1−O1	161.4(2)
Cl4−Fe3−S3	112.3(1)	S3−Mo1−O2	88.3(2)
Cl4−Fe3−S4	115.0(1)	Cl2−Mo1−S1	88.72(9)
S1−Mo1−S2	102.4(1)	Cl2−Mo1−S2	160.5(1)
S1−Mo1−S3	103.0(1)	Cl2−Mo1−S3	89.4(1)
S1−Mo1−O1	91.6(1)	Cl2−Mo1−O1	79.3(2)
S1−Mo1−O2	164.5(2)	Cl2−Mo1−O2	80.7(2)
S1−Fe2−S2	106.8(1)	Cl3−Fe2−S1	113.1(1)
S1−Fe2−S4	104.3(1)	Cl3−Fe2−S2	112.7(1)
S1−Fe3−S3	106.5(1)	Cl3−Fe2−S4	115.4(1)
Fe1−S2−Fe2	73.7(1)	Cl4−Fe3−S1	114.7(1)
Fe1−S3−Fe3	74.1(1)	S3−Fe1−S4	103.4(1)
Fe1−S4−Fe2	73.4(1)	S2−Fe3−S4	103.2(1)
Fe1−S4−Fe3	73.8(1)	O1−Mo1−O2	75.4(2)
Fe2−S1−Fe3	73.7(1)	O1−Cla−Cl	117(1)
Fe2−S4−Fe3	73.5(1)	O1a−C1−O2	124.5(6)
Cl1−Fe1−S2	111.1(1)	O1a−C1−C1a	117(1)
Cl1−Fe1−S3	114.2(1)	O2−C1−C1a	118.7(8)
Cl1−Fe1−S4	115.3(1)		

cubanes of ~2.06 Å.[20,21e] All the C−O bonds of the oxalate are equivalent, as expected, at 1.26(2) Å. The oxalate C−C bond at 1.526(9) Å precludes any double bond character and is comparable to the C−C bond of oxalic acid[48] or the oxalate ion,[49] 1.560 Å. The O−Mo−O angle at 75.4(2)° is similar to values found for the other oxalate clusters reported in this paper (*vide infra*).

$(Et_4N)_3[(MoFe_3S_4Cl_4)(C_2O_4)]$ (4). The metal−sulfur core of this compound (Figure 3, upper part) exhibits metric features (Table 6) almost identical to its parent double cubane, **4**. The main differences lie on the C═O(carbonyl) bond distances, 1.23(1) Å, clearly indicating double bond character. The sixth coordination site of the Mo atom is occupied by a Cl^- forming a very long bond with Mo, at 2.525(3) Å, one of the longest such distances known. It is outside the Mo(II−V)−Cl range (2.39−2.48 Å)[50] and perhaps too long for Mo^{3+}, the formal oxidation state usually associated with the $[MoFe_3S_4]^{3+}$ core.

$(Et_4N)_3[MoFe_3S_4Cl_3(C_2O_4)(CN)]$ (5). The crystal structure (Figure 3, lower part) shows the trianion as a single cubane possessing crystallographically required C_s symmetry. Three of the coordination sites on the Mo atom are occupied by the core sulfides, and the other three, by the terminal oxalate oxygens and the cyanide ligand. The Mo−C bond at 2.192(15) Å, typical for Mo(III−IV) cyanide complexes,[39] and the almost linear Mo−C−N angle of 178.61(13)° are comparable to values reported for $[MoFe_3S_4(SEt)_3(Cl_4\text{-cat})(CN)]^{3-}$, at 2.194(25) Å and 178.1(22)°, respectively.[20d] Selected bond distances and angles in **5** are compiled in Table 6.

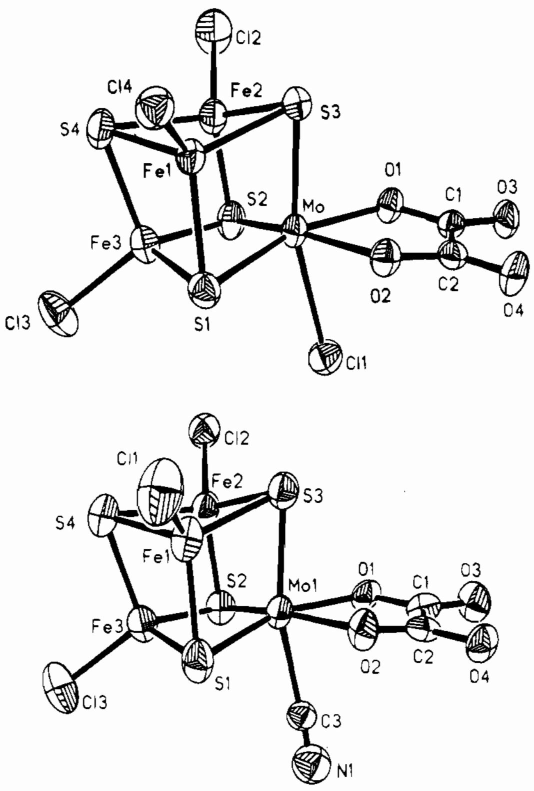

Figure 3. Structures of $[(MoFe_3S_4Cl_4)(C_2O_4)]^{3-}$, anion of **4** (upper), and $[(MoFe_3S_4Cl_3)(CN)(C_2O_4)]^{3-}$, anion of **5** (lower), showing the atom-labeling scheme. Thermal ellipsoids as drawn by ORTEP represent 40% probability surfaces.

$(Et_4N)_5\{[(MoFe_3S_4Cl_2)(C_2O_4)]_2(\mu\text{-}S)(\mu\text{-}CN)\}$ (6). The pentaanion in **6** is a doubly-bridged double cubane with a CN^- bridging end-on the two Mo atoms and a S^{2-} bridging two Fe atoms (Figure 4). The C and N atoms of the cyanide bridge are nearly impossible to differentiate and are very likely positionally disordered. Selected metric features of **6** are included in Table 7. Among the outstanding structural features in **6** are included long Mo··Mo and Fe··Fe(intercube) distances of 5.267(5) and 3.443(7) Å, respectively, and a Fe−μ_2-S−Fe angle of 104.1(4)°. The Mo−C, Mo−N, and C−N bond lengths are found at 2.25(3), 2.30(3), and 1.02(4) Å, respectively. The Mo−C(N)−N(C) angle of 157(3)° (161(3)°) significantly diverges from linearity. The Fe−μ_2-S−Fe angle and the intercube Fe··Fe distance in **6** are similar to those reported for the $[(Fe_4S_4Cl_3)_2(\mu_2\text{-}S)]^{4-}$ singly-bridged double cubane[32] at 102.2(2)° and 3.433(4) Å, respectively. In the doubly-bridged double cubanes of the general type $\{[MoFe_3S_4Cl_2(Cl_4\text{-cat})]_2(\mu_2\text{-}S)(\mu_2\text{-}X)\}^{n-}$ [21f,g] with monoatomic bridges the Fe−μ_2-S−Fe angles are more accute and the Mo··Mo and Fe··Fe separations are shorter than those in **6**. Thus, for X = OH^-, *n*

---

(48) Cox, E. G.; Dougill, M. W.; Jeffrey, G. A. *J. Chem. Soc.* **1952**, 4854.

(49) (a) Jeffrey, G. A.; Parry, G. S. *J. Chem. Soc.* **1952**, 4864. (b) Jeffrey, G. A.; Parry, G. S. *J. Am. Chem. Soc.* **1954**, *76*, 5283.

(50) (a) Nardelli, M.; Pelizzi, G.; Predieri, G. *Gazz. Chim. Ital.* **1980**, *110*, 375. (b) Garner, C. D.; Hill, L. H.; Mabbs, F. E.; McFadden, D. L.; McPhail, A. T. *J. Chem. Soc., Dalton Trans.* **1977**, 853. (c) Bird, P. H.; Wickramasinghe, W. A. *Can. J. Chem.* **1981**, *59*, 2879. (d) Yamanouchi, K.; Yamada, S.; Enemark, J. H. *Inorg. Chim. Acta* **1984**, *85*, 129. (e) Beyendorff-Gulba, G.; Strahle, J.; Liebelt, A.; Dehnicke, K. *Z. Anorg. Allg. Chem.* **1981**, *483*, 26. (f) Chou, C. Y.; Huffman, J. C.; Maatta, E. A. *J. Chem. Soc., Chem. Commun.* **1984**, 1184. (g) Butcher, R. J.; Penfold, B. R.; Sinn, E. *J. Chem. Soc., Dalton Trans.* **1977**, 853.

Table 6. Selected Bond Distances (Å) and Angles (deg) of **4** and **5**

	4	**5**
	Bond Distances	
Mo−Fe1	2.758(2)	2.743(2)
Mo−Fe2	2.735(2)	2.721(2)
Mo−Fe3	2.768(2)	2.755(2)
Mo−S3	2.367(3)	2.393(4)
Mo−S2	2.354(3)	2.339(4)
Mo−S1	2.348(3)	2.331(4)
Mo−Cl4/C3	2.525(3)	2.189(15)
Mo−O1	2.125(6)	2.135(8)
Mo−O2	2.135(6)	2.138(8)
Fe1−Fe2	2.717(2)	2.717(3)
Fe1−Fe3	2.726(2)	2.731(3)
Fe1−S3	2.253(3)	2.271(4)
Fe1−S4	2.288(3)	2.278(4)
Fe1−S1	2.261(3)	2.248(5)
Fe1−Cl1	2.224(3)	2.200(5)
Fe2−Fe3	2.726(2)	2.692(3)
Fe2−S3	2.280(3)	2.260(4)
Fe2−S4	2.281(3)	2.284(4)
Fe2−S2	2.261(3)	2.266(4)
Fe2−Cl2	2.215(3)	2.226(4)
Fe3−S4	2.275(3)	2.280(5)
Fe3−S2	2.279(3)	2.271(4)
Fe3−S1	2.285(3)	2.274(4)
Fe3−Cl3	2.214(3)	2.216(4)
O1−C1	1.288(10)	1.309(14)
O3−C1	1.220(10)	1.202(14)
O2−C2	1.273(10)	1.292(14)
O4−C2	1.227(10)	1.195(13)
C1−C2	1.566(13)	1.551(18)
C3−N1		1.041(15)
	Angles	
S3−Mo1−S2	102.4(1)	102.7(1)
S3−Mo1−S1	102.1(1)	102.2(1)
S2−Mo1−S1	102.6(1)	102.6(1)
S3−Mo1−O1	85.9(2)	88.2(2)
S2−Mo1−O1	90.8(2)	90.0(2)
S1−Mo1−O1	162.4(2)	161.3(2)
S3−Mo1−O2	87.9(2)	86.8(3)
S2−Mo1−O2	162.0(2)	161.7(2)
S1−Mo1−O2	89.4(2)	90.3(3)
O1−Mo1−O2	75.1(2)	74.5(3)
S3−Mo1−Cl5/C3	165.5(1)	166.4(4)
S2−Mo1−Cl5/C3	85.6(1)	86.0(4)
S1−Mo1−Cl5/C3	87.7(1)	85.8(4)
O1−Mo1−Cl5/C3	81.9(2)	81.3(4)
O2−Mo1−Cl5/C3	81.4(2)	82.1(5)
Mo1−O1−C1	118.3(6)	119.2(8)
Mo1−O2−C2	117.9(6)	118.8(8)
O1−C1−O3	126.0(9)	125(1)
O1−C1−C2	113.1(8)	113(1)
O3−C1−C2	120.8(8)	123(1)
O2−C2−O4	124.6(9)	126(1)
O2−C2−C1	114.4(8)	114(1)
O4−C2−C1	121.0(8)	120(1)
Mo1−C3−N1		179(2)

= 5, the corresponding values are 97.8(8)°, 4.248(5) Å, and 3.35(1) Å and for X = S^{2-}, n = 6, values of 98.7(8)°, 4.926(8) Å, and 3.33(2) Å have been reported.[21f] The structure of the pentaanion in **6** is quite similar to the {[MoFe$_3$S$_4$Cl$_2$(Cl$_4$-cat)]$_2$(μ_2-S)(μ_2-X)}$^{n-}$ anions[21g] (X = CN$^-$, n = 5, and X = N$_2$H$_4$, n = 4). For the latter atomic connectivity was established from structure determinations that were carried out using insufficient data, due to the marginal quality of the crystals.

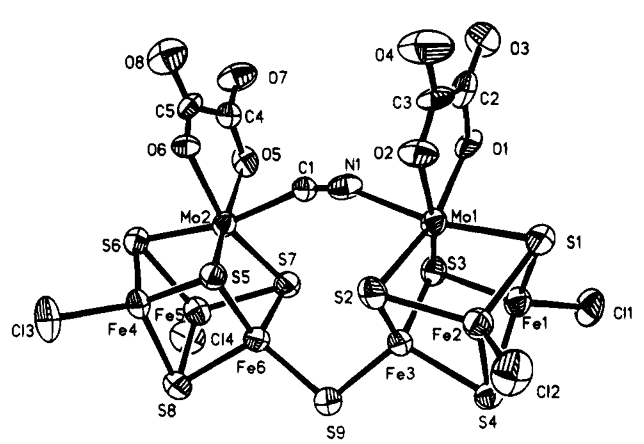

Figure 4. ORTEP plot of the {[(MoFe$_3$S$_4$Cl$_2$)(C$_2$O$_4$)]$_2$(μ_2-S)(μ_2-CN)}$^{5-}$ cluster, anion of **6**. Thermal ellipsoids as drawn by ORTEP represent 40% probability surfaces.

Table 7. Selected Bond Distances (Å) and Angles (deg) of **6**

	Bond Distances		
Mo1···Mo2	5.267(4)	O1−C2	1.316(45)
Fe3···Fe6	3.443(7)	O3−C2	1.223(45)
Mo1−O1	2.093(21)	O5−C4	1.249(45)
Mo1−O2	2.112(25)	O7−C4	1.221(45)
Mo1−N1	2.292(26)	N1−C1	1.027(42)
Mo2−O5	2.155(22)	C4−C5	1.576(48)
Mo2−O6	2.129(22	O2−C3	1.255(47)
Mo2−C1	2.250(32)	O4−C3	1.287(50)
Fe3−S9	2.169(10)	O6−C5	1.230(45)
Fe6−S9	2.201(10)	O8−C5	1.233(50)
C2−C3	1.556(47)		
	Angles		
S1−Mo1−O1	85.8(6)	S5−Mo2−O6	92.3(6)
S3−Mo1−O1	92.7(6)	S7−Mo2−O6	160.3(6)
S1−Mo1−O2	90.6(7)	S6−Mo2−C1	168.0(8)
S3−Mo1−O2	161.7(7)	O5−Mo2−C1	84.1(10)
S2−Mo1−N1	89.2(7)	S6−Mo2−O5	89.8(6)
O1−Mo1−N1	81.6(8)	S6−Mo2−O6	87.3(6)
S2−Mo1−O1	160.7(6)	O5−Mo2−O6	74.7(8)
S2−Mo1−O2	85.9(7)	S6−Mo2−C1	168.0(8)
O1−Mo1−O2	76.4(8)	S7−Mo2−C1	87.2(8)
S1−Mo1−N1	167.2(7)	O6−Mo2−C1	81.1(10)
S3−Mo1−N1	79.5(7)	Fe3−S9−Fe6	104.1(4)
O2−Mo1−N1	84.4(9)	Mo1−N1−C1	157.2(26)
S5−Mo2−O5	160.9(7)	Mo2−C1−N1	160.8(28)
S7−Mo2−O5	88.4(6)		

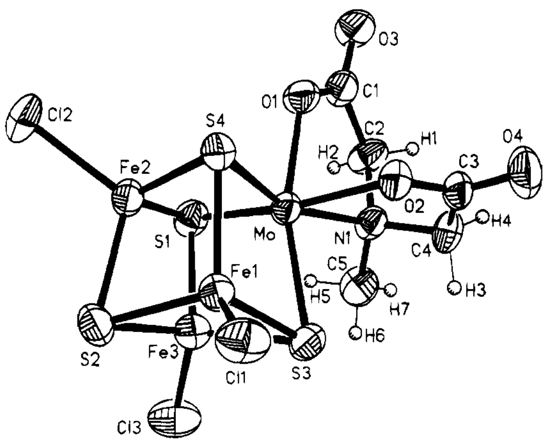

Figure 5. Structure and labeling of the [(MoFe$_3$S$_4$Cl$_3$)(mida)]$^{2-}$ single cubane, anion of **11**. Thermal ellipsoids as drawn by ORTEP represent the 40% probability surfaces.

(Et$_4$N)$_2$[MoFe$_3$S$_4$Cl$_3$(mida)] (11). The molecular structure of **11** (Figure 5) shows the single MoFe$_3$S$_4$ cubane core with intracubane metal−metal and metal−sulfur distances and other geometrical features similar to the structures discussed thus far. The three sites of the Mo atom, external to the cubane, are occupied by two carboxylate ligands and the N atom from the imino function of the (methylimino)diacetate tridentate chelate. The two Mo−O(carboxylate) distances (Table 8) are nearly identical at 2.102(8) and 2.096(7) Å, typical for metal−

Table 8. Selected Bond Distances (Å) and Angles (deg) of **11**

Bond Distances			
Mo−Fe1	2.729(2)	Fe1−S4	2.270(3)
Mo−Fe2	2.725(2)	Fe2−Fe3	2.707(2)
Mo−Fe3	2.737(2)	Fe2−Cl2	2.236(3)
Mo−S1	2.348(3)	Fe2−S1	2.263(3)
Mo−S3	2.362(3)	Fe3−S3	2.268(3)
Mo−S4	2.334(3)	Fe2−S4	2.256(3)
Mo−O1	2.102(8)	Fe3−Cl3	2.208(4)
Mo−O2	2.096(7)	Fe3−S1	2.264(4)
Mo−N1	2.292(7)	Fe3−S3	2.268(3)
Fe1−Fe2	2.763(2)	Fe3−S2	2.284(3)
Fe1−Fe3	2.730(2)	O1−C1	1.268(12)
Fe1−Cl1	2.234(3)	O3−C1	1.250(15)
Fe1−S2	2.277(3)	O2−C3	1.293(12)
Fe1−S3	2.267(3)	O4−C3	1.215(14)
N1−C2	1.491(15)	N1−C4	1.509(13)
N1−C5	1.541(13)	C1−C2	1.525(14)
C3−C4	1.484(14)		
Angles			
S1−Mo−O1	86.2(2)	Mo−N1−C4	106.7(5)
S4−Mo−O1	88.8(2)	Mo−N1−C5	116.3(6)
S1−Mo−O2	162.6(2)	C4−N1−C5	107.6(7)
S4−Mo−O2	87.9(2)	O1−C1−C2	117.4(10)
S3−Mo−N1	88.6(2)	N1−C2−C1	112.2(8)
O1−Mo−N1	76.5(3)	O2−C3−C4	116.8(9)
S1−Mo−S3	102.3(1)	N1−C4−C3	112.5(8)
S1−Mo−S4	103.0(1)	Mo−N1−C2	107.8(5)
S3−Mo−O1	162.9(2)	C2−N1−C4	110.1(8)
S3−Mo−O2	88.0(2)	C2−N1−C5	108.3(8)
O1−Mo−O2	80.4(3)	O1−C1−O3	122.7(9)
S1−Mo−N1	90.1(2)	O3−C1−C2	119.8(9)
S4−Mo−N1	159.7(2)	O2−C3−O4	123.0(9)
O2−Mo−N1	76.1(3)	O4−C3−C4	120.0(9)
Mo−O2−C3	121.1(6)		

carboxylate moieties. The coordination environment of the six-coordinate, distorted octahedral Mo atom is completed with the N atom of the ligand at a distance of 2.292(7) Å. This bond is slightly shorter from the corresponding Mo−N bond in K_3-$[Mo^{VI}O_3(\text{nitrilotriacetato})\cdot H_2O]$,[42c] at 2.388(5) Å. Other bond distances within the mida ligand are unremarkable. The coordination around the Mo atom in **11** is similar to the coordination of the Mo atom in nitrogenase,[13,14] and the reactivity of **11** in the catalytic reductions of hydrazine and acetylene is presently under investigation.

Proposed Structure of $(Et_4N)_3[MoFe_3S_4Cl_3(Hcit)]$ (7). The lack of adequate quality crystals of **7** for single crystal X-ray measurements led us to seek alternative ways to deduce the possible coordination mode of the citrate ligand to the Mo atom. The principal studies carried out and the results associated with them are as follows: (a) Far-infrared spectroscopic results (see Experimental Section) are satisfactorily consistent with a cuboidal $MoFe_3S_4$ core. The spectrum exhibits core skeletal vibrations comparable (albeit not identical) to spectra obtained in our laboratory on numerous Mo/Fe/S clusters.[24,31] (b) The Mössbauer spectrum (obtained at 125 K *vs* Fe metal) consists of a broad asymmetric quadruple double with average values of isomer shift and quadrupole splitting of 0.37 and 0.85 mm/s, respectively. These values are in accordance with 2Fe(III) + Fe(II) formal oxidation states and typical for the $[MoFe_3S_4]^{3+}$ core found in a plethora of other clusters with the same core. (c) The EPR spectrum of **7** (in CH_3CN, at 4 K) is consistent with a $S = {}^3/_2$ ground state and with g values ($g_{max} = 5.403$, $g_x = 2.463$, and $g_{min} = 1.772$) comparable to those reported for other $MoFe_3S_4$ cubane clusters.[23b,51] For comparison, the EPR spectra of **1**, **8**, and **11** (Figure 6) obtained under identical conditions also show $S = {}^3/_2$ ground states. For these clusters the values of g_{max}, g_x, and g_{min} are 5.403, 2.463, and 1.903 for **1**, 5.317, 2.519, and 1.851 for **8**, and 4.467, 2.608, and 1.882 for **11**. (d) The cyclic voltametric traces of **7** in CH_2Cl_2 consist of well-defined waves: a *single* reduction at −1050 mV and *single* oxidation at +260 mV *vs* Ag/AgCl. Single reduction waves are typical for single $[MoFe_3S_4]^{3+}$ cubane cores, whereas, in the cases of bridged cubane subunits, at least doubling of the reduction waves occurs.[24a,21b,43] Dimerization in the case of **7** therefore seems unlikely. (e) Analytical studies conducted on highly crystalline samples of **7** are consistent with the formulation 3:1:1 Et_4N^+:$MoFe_3S_4$ cubane unit:citrate (triply deprotonated).[52] (f) The carbonyl region of the mid-infrared spectrum of **7** shows a medium to strong band at 1720 cm^{-1}, assigned to a noncoordinated, protonated −COOH moiety.[40b] This band completely vanishes upon reaction of **7** with (Et_4N)-OH, and a new strong stretch at 1597 cm^{-1} emerges, not inconsistent with ionic $-COO^-$. Also, the $\nu_{sym}(C-O)$ seems perturbed and gives rise to a doublet at 1379 and 1388 cm^{-1}. Δ values conform with an ionic $-COO^-$ moiety, and the $\nu(O-H)$ stretch at 3543 cm^{-1} disappears. Metal complexes of the type M−Hcit, having free −COOH group(s), have been structurally characterized.[53] (g) Only one O−H stretch was observed in the vibrational spectrum, at 3543 cm^{-1} (only in highly crystalline samples), assigned to the free −COOH group mentioned above. The hydroxyl group of the citrato ligand seems to be deprotonated. This behavior of the −OH group has been fully recognized by the reduction of its pK_a value upon its coordination to a transition metal ion.[54] On the basis of the data available, we propose that **7** and **8** contain $[MoFe_3S_4]^{3+}$ cubic cores with Cl^- ligands bound to the Fe sites. The citrate is attached to the Mo site in a tridentate fashion through two of its carboxyl groups (the central and the terminal ones) and the *deprotonated* hydroxyl group for **7** or a *protonated* hydroxyl

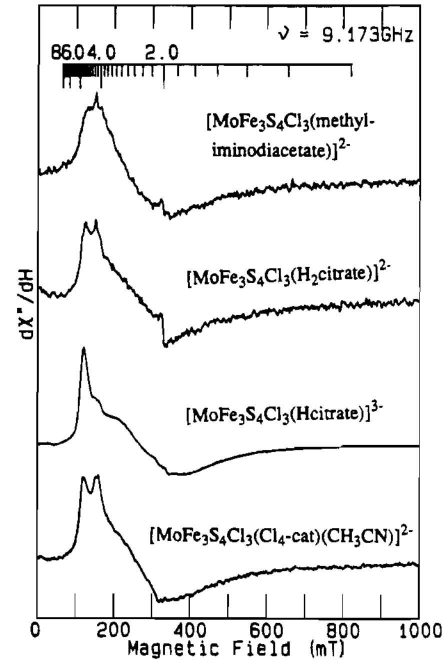

Figure 6. EPR spectra of clusters **1**, **7**, **8**, and **11**, in CH_3CN glasses at 4 K.

---

[51] Armstrong, W. H.; Mascharak, P. K.; Holm, R. H. *Inorg. Chem.* **1982**, *21*, 1699.

[52] Various formulations were tested as potential candidates for the exact identity of the compound. Only the one described herein was consistent with *all* the spectroscopic information in our hands.

[53] (a) Job, R.; Kelleher, P. J.; Stallings, W. C.; Monti, C. T.; Glusker, J. P. *Inorg. Chem.* **1982**, *21*, 3760. (b) Flanagan, J.; Griffith, W. P.; Skapski, A. C.; Wiggins, R. W. *Inorg. Chim. Acta* **1985**, *96*, L23. (c) Djordjevic, C.; Lee, M.; Sinn, E. *Inorg. Chem.* **1989**, *28*, 719.

Scheme 1

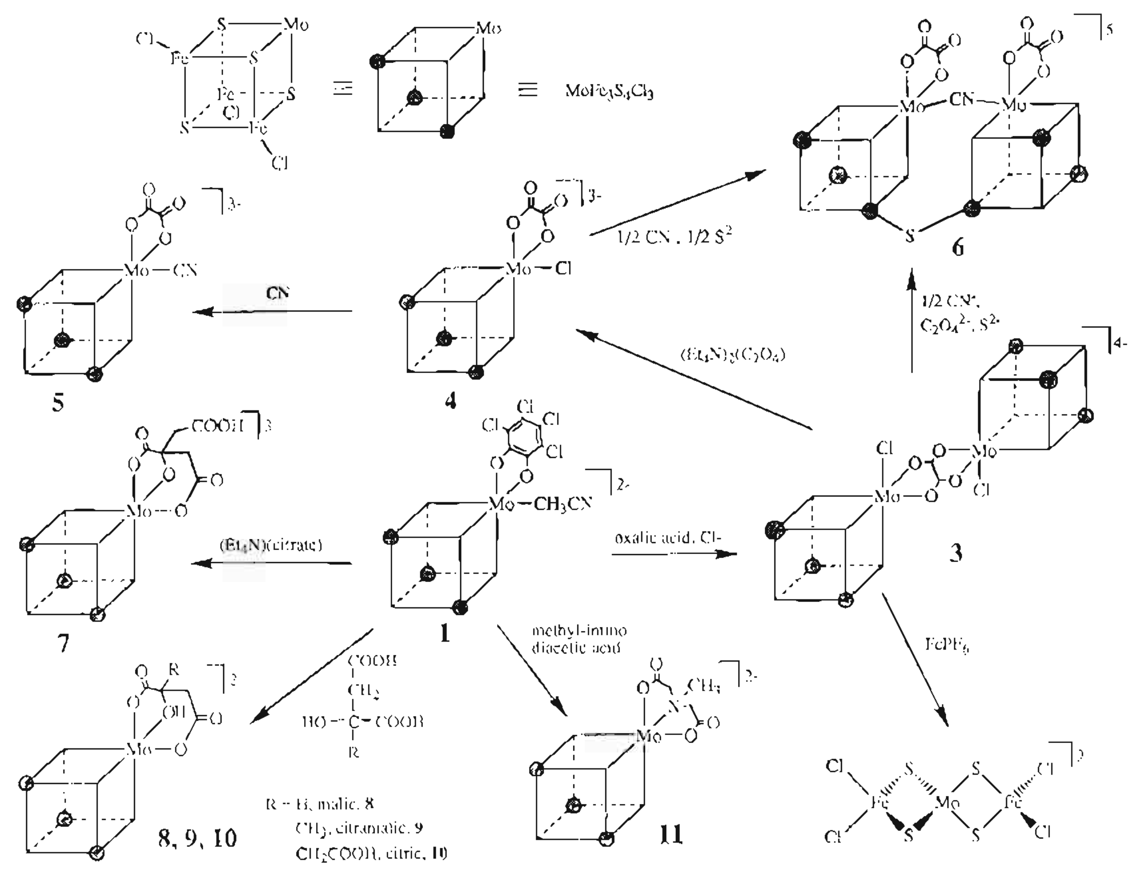

group for **8**. This is the most common coordination mode of citrate to metals and has numerous precedents among transition metal complexes.[55]

Reactivity. The reactivity and cluster interconversions are summarized in Scheme 1. The ability of the oxalate ligand to undergo a two electron oxidation with production of CO$_2$ is well-known:[56]

$$C_2O_4^{2-} \rightarrow 2CO_2 + 2e^-$$

This oxidation apparently takes place in the reaction of **3** with 2 equiv of [Fe(Cp)$_2$]PF$_6$ in CH$_3$CN or DMF solution. In this reaction the MoFe$_3$S$_4$ cubane structure colapses, and the linear trimer,[26] Cl$_2$FeS$_2$MoS$_2$FeCl$_2^{2-}$, is produced in moderate yield. The presence of anionic ligands such as Cl$^-$, Br$^-$, or I$^-$ do not prevent the decomposition of the cluster. The reaction of **3** with a 1:1 mixture of tetrachloro-1,2-benzoquinone and the tetrachlorocatecholate dianionic ligand affords **1** in good yields. In this redox process the Mo-bound chloride in **3** dissociates following oxidation of the oxalate ligand and is replaced by the coordinating solvent (CH$_3$CN). The reaction of **4** with a stoichiometric amount of tetrachloro-1,2-benzoquinone in CH$_3$CN affords **1** in low yields. The Cl$^-$ ligands in **3** and **4** (as suggested by the long Mo–Cl bond lengths) are labile and, upon reaction with N$_3^-$, CN$^-$, or N$_2$H$_4$, produce clusters with Mo-bound azide (ν(N–N) 2051 cm^{-1}), cyanide (ν(C≡N) 2080 cm^{-1}), and hydrazine (ν(N–H) 3294, 3235, 3160 cm^{-1} and $\nu_{\rm twist}$(N–H) 1160 cm^{-1}), respectively. The oxalate cubanes are totally unreactive toward oxidation by reagents such as S$_8$, BzSSSBz, or organic disulfides. A variety of MoFe$_3$S$_4$ clusters exhibit catalytic activity in the reduction of hydrazine (a nitrogenase substrate[57]) to ammonia (or NH$_4^+$)[58] with cobaltocene and 2,6-lutidine hydrochloride as sources of electrons and protons, respectively:

$$N_2H_4 + 2e^- + 4H^+ \rightarrow 2NH_4^+$$

Cluster **1** catalyzes the above reduction (substrate:catalyst ratio 100:1) with a 34% yield in 0.5 h. Cluster **11** under identical conditions gives a 63% yield. Finally, clusters **7** and **8** carry out this reaction in 92% yield. Detailed aspects of the reactivity

---

(54) (a) Grzybowski, A. K.; Tate, S. S.; Datta, S. P. *J. Chem. Soc. A* **1970**, 241. (b) Hamm, R. E.; Shull, C. M.; Grant, D. M. *J. Am. Chem. Soc.* **1954**, *76*, 2111. (c) Patnaik, R. K.; Pani, S. *J. Indian Chem. Soc.* **1957**, *34*, 619. (d) Shnarevich, A. I. *Russ. J. Inorg. Chem.* **1963**, *8*, 1083. (e) Strouse, J.; Layten, S. W.; Strouse, C. E. *J. Am. Chem. Soc.* **1977**, *99*, 562. (f) Strouse, J. *J. Am. Chem. Soc.* **1977**, *99*, 572. (g) Shweky, I.; Bino, A.; Goldberg, D. D.; Lippard, S. J. *Inorg. Chem.* **1994**, *33*, 5161.

(55) (a) Glusker, J. P.; Carrell, H. L. *J. Mol. Struct.* **1973**, *15*, 151. (b) Alcock, N. W.; Dudek, M.; Grybos, R.; Hodorowicz, E.; Kanas, A.; Samotus, A. *J. Chem. Soc., Dalton Trans.* **1990**, 707. (c) Quiros, M.; Goodgame, D. M. L.; Williams, D. J. *Polyhedron* **1992**, *11*, 1343. (d) Herrmann, W. A.; Herdweck, E.; Pajdla, L. *Inorg. Chem.* **1991**, *30*, 2579. (e) Asato, E.; Driessen, W. L.; de Graaff, R. A. G.; Hulsbergen, F. B.; Reedijk, J. *Inorg. Chem.* **1991**, *30*, 4210. (f) Herrmann, W. A.; Herdweck, E.; Pajdla, L. *Z. Kristallogr.* **1992**, *198*, 257. (g) Cruywagen, J. J.; Saayman, L. J.; Niven, M. L. *J. Crystallogr. Spectrosc. Res.* **1992**, 22, 737. (h) Llopis, E.; Ramirez, J. A.; Domenech, A.; Cervilla, A. *J. Chem. Soc., Dalton Trans.* **1993**, 1121. (i) Asato, E.; Katsura, K.; Mikuriya, M.; Fujii, T.; Reedijk, J. *Inorg. Chem.* **1993**, *32*, 5322.

(56) (a) Paonessa, R. S.; Trogler, W. C. *Inorg. Chem.* **1983**, 22, 1038. (b) Paonessa, R. S.; Prignano, A. L.; Trogler, W. C. *Organometallics* **1985**, *4*, 647. (c) Ham, E. K.; West, R. *Organometallics* **1990**, *9*, 1517. (d) Anderson, J. E.; Murphy, C. P.; Real, J.; Balué, J.; Bayón, J. C. *Inorg. Chim. Acta* **1993**, *209*, 151. (e) Vos, A.; Mullens, J.; Yperman, J.; Franco, D.; Van Poucke, L. C. *Eur. J. Solid State Inorg. Chem.* **1993**, *30*, 929.

(57) Thorneley, R. N. F.; Lowe, D. J. *Biochem. J.* **1984**, *224*, 887.

(58) Coucouvanis, D.; Mosier, E. M.; Demadis, K. D.; Patton, S.; Malinak, S. M.; Kim, C. G.; Tyson, A. M. *J. Am. Chem. Soc.* **1993**, *115*, 12193.

of the Mo-bound polycarboxylate $MoFe_3S_4$ clusters will appear in a future publication.[59]

Summary and Conclusions

(1) A variety of double (**3, 6**) and single (**4, 5, 7–11**) cubanes have been successfully synthesized from the common precursor **1**. In **1** the Cl_4-cat ligand can be protonated by appropriate polycarboxylic acids (or in some instances mercapto–carboxylic acids),[60] yielding Mo-coordinated single or double cubanes. These are the first examples of Mo/Fe/S clusters that show a polycarboxylate ligand coordinated to the Mo atom.

(2) The structures of **3–4** and **11** have been determined. The $MoFe_3S_4$ cores within these clusters are similar to examples reported in the literature.[20,21] Mo–O(oxalate) bond distances are 2.207(7) Å for the bridging oxalate and 2.082(21)–2.138(8) Å for the terminal oxalate.

(3) Ongoing studies in our laboratory are aimed toward an understanding of the effects that various polycarboxylate anions may have in the reactivity characteristics associated with the new polycarboxylate $MoFe_3S_4$ clusters. These studies indirectly may suggest a role for the homocitrate ligand in the nitrogenase cofactor.

Acknowledgment. The authors thank Dr. W. R. Dunham for obtaining the EPR spectra shown in Figure 6 and the Mössbauer spectrum of compound **7**. The support of this work by a grant from the National Institutes of Health (GM-33080) is gratefully acknowledged.

Supplementary Material Available: Table S1, containing a listing of positional parameters, thermal parameters, and selected bond distances and angles for $(Et_4N)_2[MoFe_3S_4Cl_3(mida)]$, **11** (7 pages). Ordering information is given on any current masthead page. Listings of positional parameters, thermal parameters, selected bond distances and angles, and calculated and observed structure factors for **3–6** have been deposited as supplementary material with previous publications.[24a,b]

IC941254M

---

[59] Demadis, K. D.; Coucouvanis, D. Manuscript in preparation.

[60] Clusters of the general type $[MoFe_3S_4Cl_3(SCH(R)COO)]_2^{4-}$ (R = H, mercaptoacetate; R = CH_3, thiolactate; R = CH_2COOH, thiomalate) have now been structurally characterized and shown to catalyze the reduction of hydrazine to ammonia: Demadis, K. D.; Coucouvanis, D. *Inorg. Chem.* **1994**, *33*, 4195.